Published in *Dalton Trans.*, 2022,51, 12080-12099
DOI: 10.1039/d2dt01558g

Heterobimetallic μ_2-Halocarbyne complexes

Liam K. Burt,[a] Rian D. Dewhurst,[a-c] Anthony F. Hill,[a,*] Richard Y. Kong,[a] Emily E. Nahon,[a] and Chee S. Onn[a]

Received 00th January 20xx,
Accepted 00th January 20xx

DOI: 10.1039/x0xx00000x

The halocarbyne complexes $[M(\equiv CX)(CO)_2(Tp^*)]$ (M = Mo, W; X = Cl, Br; Tp* = hydrotris(dimethylpyrazolyl)borate) react with $[AuCl(SMe_2)]$, $[Pt(\eta^2\text{-}H_2C{=}CH_2)(PPh_3)_2]$ or $[Pt(\eta^2\text{-nbe})_3]$ (nbe = norbornene) to furnish rare examples of μ_2-halocarbyne complexes $[MAu(\mu_2\text{-}CX)Cl(CO)_2(Tp^*)]$, $[MPt(\mu_2\text{-}CCl)(CO)_2(PPh_3)_2(Tp^*)]$ and $[W_2Pt(\mu_2\text{-}CCl)_2(CO)_4(Tp^*)_2]$. The complex $[WPt(\mu_2\text{-}CCl)(CO)_2(PPh_3)_2(Tp^*)]$ rearranges slowly in refluxing toluene to the μ_2-carbido complex $[WPt(\mu_2\text{-}C)Cl(CO)_2(PPh_3)_2(Tp^*)]$, however this transformation occurs spontaneously during silica-gel chromatography. One phosphine ligand of $[WPt(\mu_2\text{-}CCl)(CO)_2(PPh_3)_2(Tp^*)]$ is readily substituted by CO to afford $[WPt(\mu_2\text{-}CCl)(CO)_3(PPh_3)(Tp^*)]$. These μ_2-halocarbyne complexes have been interrogated by spectroscopic, crystallographic and computational methods, the latter by reference to data for terminal halocarbyne precursors $[M(\equiv CX)(CO)_2(Tp^*)]$.

Introduction

To date there has been considerable advancement in *C*-functionalised carbyne chemistry. The focus has, however, been primarily on those bearing hydrocarbyl substituents relevant to the emergence of alkyne metathesis technologies.[1] Those bearing heteroatoms are somewhat less-studied, not least because with the exception of amino-[2] and silyl-carbynes,[3] traditional Fischer-type synthetic protocols[4] are not suitable. An extensive chemistry was developed by Angelici for thiolatocarbynes derived *via* thiocarbonyl alkylation[4a,5] and alternative access is afforded *via* attack at halocarbynes by chalcogenolate nucleophiles.[6] Lalor's halocarbynes $[M(\equiv CX)(CO)_2(Tp^*)]$ (M = Mo, W; X = Cl, Br, Chart 1),[6a] have also allowed the development of pnictogen-functionalised carbynes[7-9] either *via* nucleophilic halide substitution (spontaneous or palladium-mediated)[8,9] or alternatively *via* lithium-halogen exchange to afford $[M(\equiv CLi)(CO)_2(Tp^*)]$.[10] These lithiocarbynes or their stannyl derivatives $[M(\equiv CSnR_3)(CO)_2(Tp^*)]$ (M = Mo, W; R = Me, Bu)[11] serve as nucleophiles towards a range of pnictogen-centred electrophiles.[12] The efficacy of stannyl carbynes in such processes may be augmented *via* catalytic transmetallation sequences that involve intermediate gold and palladium μ-carbido complexes. Accordingly, though limited in number,[6a,13] the synthetic utility of terminal halocarbynes $[L_nM(\equiv CX)]$ (X = Cl, Br) has been amply demonstrated.

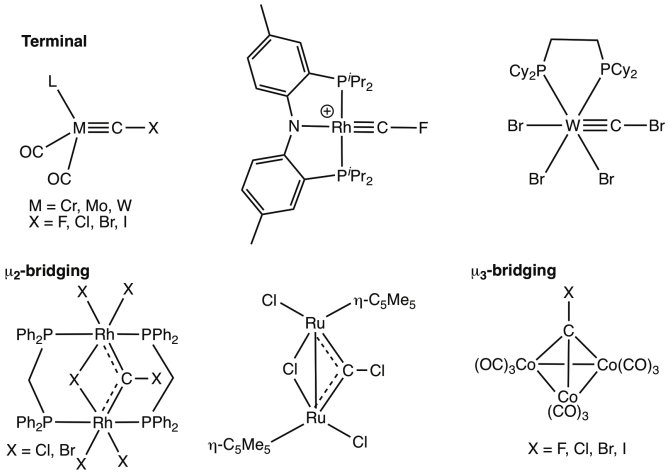

Chart 1: Representative examples of halocarbyne bonding modes (L = η-C_5R_5 R = H, Me, κ^3-Tp*.

The synthetic versatility of μ_3-halocarbyne bridged clusters is similarly well-documented, albeit over a far longer history. As first observed by Dent *et al.*, cobalt carbonyl reacted with CCl_4 to afford the chlorocarbyne complex $[Co_3(\mu_3\text{-}CCl)(CO)_9]$.[14] Alongside the bromocarbyne analogue, this complex proved to be a key synthon in the development of cobalt carbyne, ketenylidene and carbido chemistry.[15] Though less studied, μ_3-halocarbynes of group 8 metals $[Ru_3(\mu_3\text{-}CX)(\mu_2\text{-}H)_9(CO)_9]$ (X = Cl or Br) and $[Os(\mu_3\text{-}CBr)(\mu_2\text{-}H)(CO)_9]$[16] are known. Additionally, heterotrimetallic examples have been reported to arise from metal vertex substitution reactions of $[Co_3(\mu_3\text{-}CCl)(CO)_9]$, *e.g.*, $[MoCo_2(\mu_3\text{-}CCl)(CO)_8(\eta^5\text{-}C_5H_5)]$.[17] Similar fluorocarbyne clusters result from the addition of dimetal reagents $[Co_2(CO)_8]$ and $[Mo_2(CO)_6(\eta^5\text{-}C_5H_5)_2]$ to Hughes' terminal fluorocarbyne complexes $[M(\equiv CF)(CO)_2(\eta^5\text{-}C_5R_5)]$ (M = Cr, Mo, W; R = H, Me).[18] Terminal fluorocarbyne complexes themselves remain exceedingly rare, being limited to these and the pincer derivative $[Rh(\equiv CF)(PNP)]^+$ [PNP = $N(C_6H_4Me\text{-}4,P^iPr_2\text{-}2)_2$].[19] Coupled with the scarcity of terminal halocarbynes in general,[13] Stone's approach of adding extraneous metal reagents across metal-carbon mutliple bonds[20] is somewhat robbed of its potential generality.

[a.] *Research School of Chemistry, The Australian National University, Canberra, ACT 0200, Australia. Email: a.hill@anu.edu.au*
[b.] *Institute for Inorganic Chemistry, Julius-Maximilians-Universität Würzburg, Am Hubland, 97074 Würzburg, Germany.*
[c.] *Institute for Sustainable Chemistry & Catalysis with Boron, Julius-Maximilians-Universität Würzburg, Am Hubland, 97074 Würzburg, Germany.*

†Electronic Supplementary Information (ESI) available: Selected NMR spectra (PDF). See DOI: 10.1039/x0xx00000x. CCDC 2033076, 2033078 and 2173039-2173050 contain the supplementary crystallographic data for this paper, and are available free of charge from The Cambridge Crystallographic Data Centre

Bimetallic complexes with μ_2-halocarbyne ligands are limited to the structurally authenticated examples $[W_2(\mu_2\text{-CCl})Cl_7]_n$,[21a] $[Ru_2(\mu_2\text{-CCl})(\mu\text{-Cl})Cl_2(\eta^5\text{-}C_5Me_5)_2]$[21b] and $[Rh_2(\mu_2\text{-CX})(\mu_2\text{-X})X_4(\mu\text{-dppm})_2]$ (X = Cl, Br; dppm = bis(diphenylphosphino)methane).[22] The former was obtained in undisclosed yield from the pyrolysis (six weeks, 100 °C) of WCl_6, CCl_4 and arsenic.[21] While no motivation or rationale for the reaction was provided, we presume it was inspired by the standard synthesis[21c] of WCl_4 from WCl_6 and elemental phosphorus, with the CCl_4 playing an unintended role. Carbon tetrachloride plays a similar role in the recently reported reaction with $[Ru_3(\mu_3\text{-H})_2(\mu_2\text{-H})_3(\eta\text{-}C_5Me_5)_3]$ to afford $[Ru_2(\mu_2\text{-CCl})(\mu_2\text{-Cl})Cl_2(\eta\text{-}C_5Me_5)_2]$.[21b] The latter dirhodium complexes arise from the halogenation of the μ-carbido complexes $[Rh_2(\mu_2\text{-C})X_2(\mu\text{-dppm})_2]$,[22] and accordingly neither approach appears to promise any degree of generality. Beck, however, has reported that in the reaction of $[Mo(\equiv CBr)(CO)_2(Tp^*)]$ (Tp* = hydrotris(dimethylpyrazolyl)borate) with $[Pt(\eta^2\text{-}C_2H_4)(PPh_3)_2]$, the complex $[MoPt(\mu_2\text{-CBr})(CO)_2(PPh_3)_2(Tp^*)]$ is an intermediate *en route* to the μ-carbido complex $[MoPt(\mu_2\text{-C})Br(CO)_2(PPh_3)_2(Tp^*)]$ *via* insertion of platinum into the C–Br bond.[23] The addition of '$Pt(PR_3)_2$' fragments across the metal-carbon multiple bond of carbyne complexes $[M(\equiv CR)(CO)_2(L)]$ (L = $\eta\text{-}C_5H_5$, $\eta\text{-}C_5Me_5$, $\eta^5\text{-}C_2B_9H_9Me_2$) has been extensively investigated by Stone for simple alkyl, aryl and alkynyl substituted carbynes.[24] Furthermore, we have extended this to carbon wire C_2 and C_6 ditungsten systems.[25] In terms of *heteroatom*-functionalised carbynes, the approach is so far limited to Hughes' examples noted above, a boryloxy example $[WPt\{\mu_2\text{-COB(NMe}_2)B(NMe_2)C_5H_4\}(CO)_2(PPh_3)_2]$[26] and phosphonio-, phosphino-, arsino and arsoniocarbynes.[27]

It therefore seemed plausible that an investigation of the reactions of the halocarbyne complexes $[M(\equiv CX)(CO)_2(Tp^*)]$ (M = Mo, W; X = Cl, Br) with unsaturated metal centres might provide access to a variety of heterobimetallic μ_2-halocarbyne complexes. Herein we describe a range of μ_2-halocarbyne complexes arising from the reactions of these terminal halocarbynes with unsaturated d^{10} metal reagents $[Pt(\eta^2\text{-}C_2H_4)(PPh_3)_2]$, $[Pt(\eta^2\text{-nbe})_3]$ (nbe = norbornene) and $[AuCl(SMe_2)]$.

Results and Discussion

It is first useful, as a point of reference, to collate available spectroscopic and structural data for known terminal[13,14,17,18,28] and μ_2-halocarbyne[20-22] complexes (Table 1) so as to benchmark those that follow. Whilst **1c** and **1d** have been used extensively, their crystal structure determinations have not been previously reported and are therefore included here for completeness. These studies were confounded by a recurrent problem for the general class of *pseudo*-octahedral compounds of the form [MXYZ(Tp*)] (X, Y, Z = mono or diatomic ligands). The steric bulk associated with the Tp* ligand which provides kinetic protection also protrudes sufficiently that it dominates crystal packing such that the remaining ligands X, Y and Z are prone to positional disorder. To further complicate matters, when **1c** crystallises in the *P*nma space group (Figure 1) it straddles a crystallographic mirror plane (*x, ¼, z*) that includes the carbyne carbon, molybdenum, boron and unique pyrazolyl ring, but has the bromide disordered either side. Thus whilst the connectivity is in each case unambiguously established, some prudence is needed to avoid interpreting geometric features beyond what is warranted by the precision of the structural models. Similar issues were identified in some of Hughes' fluorocarbyne structures where CO/CF disorder was inferred.

Structure and Bonding: Is a Carbonyl Analogy Useful?

A further consequence of the limited studies into terminal halocarbyne complexes is that discussion of their bonding is limited to a single analysis by Hughes.[18] The fluorocarbyne cation $[CF]^+$ is isoelectronic with CO, the bonding of which to transition metals is well understood. We therefore begin from this standpoint when considering the heavier halocarbynes, whilst acknowledging that other formalisms are commonplace when assigning a notional charge to a carbyne ligand, *e.g.*, as a trianionic ligand.[29] The cationic fragment deconstruction allows the bonding to be considered as comprising σ-donation from an occupied *sp*-orbital on carbon. This occurs in synergic concert with two retrodative interactions from metal d-orbitals to the empty p_x and p_y orbitals of the $[CX]^+$ ligand. A similar approach has been used to interrogate the bonding in the heavier chalcocarbonyl analogues CA (A = S, Se, Te),[6b,30] specifically to discern any trends on descending the group.

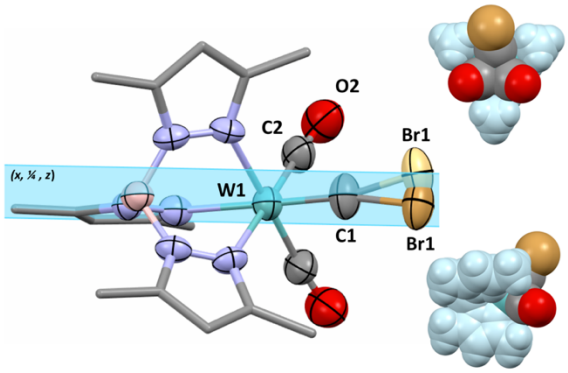

Figure 1. Molecular structure of **1c** in a crystal (50% displacement ellipsoids, pyrazoyl groups simplified and hydrogen atoms omitted, alternative disordered atoms sites not shown). Insets = space filling depiction of kinetic protection afforded by bulky Tp* ligand (pale blue).

Table 1: Spectroscopic and structural properties of η^1 and μ_2-halocarbynes.

Complex	δ_C [ppm][a]	$^1J_{CF}$ [Hz]	δ_P [ppm]	ν_{CO} [cm^{-1}][b]	k_{CO} [Ncm^{-1}]	r_{MC} [Å]	r_{CX} [Å]	M–C–X [°]	r_{MM} [Å]
Terminal Halocarbynes									
[Mo(≡CCl)(CO)$_2$(Tp*)] (**1a**)[13]	208.7			2005, 1921[c]	15.54				
[W(≡CCl)(CO)$_2$(Tp*)] (**1b**)[13]	205.6			1991, 1902[c]	15.29				
[Mo(≡CBr)(CO)$_2$(Tp*)] (**1c**)[13]	202.5			2008, 1924[c]	15.59	1.910(5)[d]	1.875(5)	163.7(3)	
[W(≡CBr)(CO)$_2$(Tp*)] (**1d**)[13c]	198.0			1994, 1905[c]	15.33	1.946(12)[d]	1.901(14)	169.4(5)	
[W(≡C-I)(CO)$_2$(Tp*)] (**1e**)[28]	183.2			1992, 1907[c]	15.33				
[Mo(≡C-I)(CO)$_2$(Tp*)] (**1f**)[13]	n.r.			2009, 1927[c]	15.62				
[Mo(≡CCl)(CO)$_2${B(pz)$_4$}] (**1g**)[13]	n.r.			2010, 1929[c]	15.65	1.893[g]	1.540	172.0	
						1.895	1.550	175.0	
						1.894	1.553	171.2	
[Mo(≡CCl)(CO)$_2${HB(pzMe$_3$)$_3$}](**1h**)[28]	208.2			2005, 1920[c]	15.54	1.798(5)	1.680(6)	165.7(4)	
[Mo(≡CBr)(CO)$_2${HB(pzMe$_3$)$_3$}](**1i**)[28]	201.9			2007, 1923	15.58				
[Cr(≡CF)(CO)$_2$(Cp*)][18]	219.7	575		2002, 1930	15.59				
[Mo(≡CF)(CO)$_2$(Cp)][18]	217.3	565		2017, 1946	15.84				
[Mo(≡CF)(CO)$_2$(Cp*)][14]	219.1	556		2002, 1930	15.59	1.971(1)	1.15(4)	177.7(1)[f]	
[W(≡CF)(CO)$_2$(Cp)][18]	220.9	532		2020, 1935	15.78				
[W(≡CF)(CO)$_2$(Cp*)][18]	223.7	538		1994, 1918	15.43	1.852(4)	1.300(6)	177.4(1)[f]	
[W(≡CBr)Br$_3$(dcpe)][17]	229.0		50.8[e]			1.793(6)	1.822(6)	171.5(4	
[Rh(≡CF)(PNP)]$^+$ [18]	n.r.	470	89.3			1.702(7)	1.257(8)	173.4(7)	
μ_2-halocarbynes									
[W$_2$(μ_2-CCl)Cl$_7$][21a]	n.r.					1.94(1), 1.94(2)	1.67(2)	139.5(8), 137.8(9)	2.561(3)
[Rh$_2$(μ_2-CCl)(μ-Cl)Cl$_4$(dppm)$_2$][22]	n.r.		3.4[e]			1.912(4), 1.947(6)	1.674(7)	125.1(3), 123.6(3)	3.1867(6)
[Rh$_2$(μ_2-CBr)(μ-Cl)Br$_4$(dppm)$_2$][22]	n.r.		-5.7[e]			2.10(4), 2.10(4)	1.57(6)	130.0(13), 130.0(13)	3.221(3)
[MoPt(μ_2-CBr)(PPh$_3$)$_2$(CO)$_2$(Tp*)] (**3c**)[23]	315.9		38.1, 25.8	1885, 1753					
[Ru$_2$(μ_2-CCl)(μ_2-Cl)Cl$_2$(η-C$_5$Me$_5$)$_2$][21b]	323.4					1.916(7), 1.929(7)	1.649(8)	135.0(4), 133.5(4)	2.7540(6)

[a]Measured in C_6D_6 unless specified otherwise. [b]Measured in *n*-hexane. [c]Measured in cyclohexane. [d]This work. [e]Measured in $CDCl_3$. [f]Halocarbyne and carbonyl ligands disordered. [g]E.s.d. values not published, three crystallographically distinct molecules.

The frontier orbitals of interest for the complete set of halocarbyne cations [CX]$^+$ (X = F, Cl, Br, I; DFT: ωB97X-D/6-31G*/LANL2Dζ(I)) are summarised in Figure 2. The five orbitals of interest comprise an occupied degenerate pair of C–X π-bonding orbitals that increase in energy with the heavier halogen substituents. The most dramatic change occurs on going from [CF]$^+$ to [CCl]$^+$. Given that at present halocarbyne complexes are limited to metals with high d-occupancies (d^6 or d^8 in the cationic carbyne description), the impact of these orbitals is secondary. The σ-donor orbital increases in energy monotonically as expected based on the electronegativities of the respective halogens, though the contribution from carbon decreases. Perhaps less expected, however, is the observation that there is rather little variation in the *energies* of the two π-acceptor orbitals down the group. In terms of the topology, however, the contributions from carbon p-orbitals decrease steadily. This contrasts with what is observed for the isoelectronic chalcocarbonyl series for which the π-acidity of the diatomic increases steadily and quite significantly. Taken together, the molecular orbitals for the halocarbyne cations indicate that the synergic bonding of these ligands to a transition metal will result in a progressively more electron-rich metal centre upon descending group 17. The superlative π-acidity of fluorocarbyne ligands would certainly appear to be substantiated by ν_{CO}-associated infrared data for Hughes' complexes [M(≡CF)(CO)$_2$(η^5-C$_5$R$_5$)][18] which suggest comparable π-acidity for [CF]$^+$ and [NO]$^+$ ligands, *e.g.*,

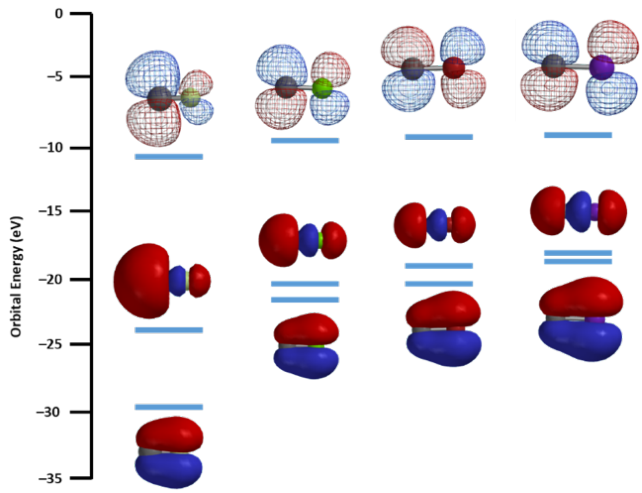

Figure 2. Calculated {DFT: ωB97X-D/6-31G*/LANL2Dζ} energy levels of frontier orbitals of interest for halocarbyne cations CX$^+$ {from left to right: X = F, Cl, Br, I}.

[Cr(≡CF)(CO)$_2$(η^5-C$_5$Me$_5$)] (ν_{CO} = 2002, 1930 cm^{-1}, k_{CO} = 15.61 Ncm^{-1}) *cf.* [Cr(NO)(CO)$_2$(η^5-C$_5$Me$_5$)] (ν_{CO} = 2000, 1930 cm^{-1}, k_{CO} = 15.59 Ncm^{-1}).[31] There is a lack of confluence between metal-ligand sets employed for Hughes' fluorocarbynes (η^5-C$_5$R$_5$) and Lalor's chloro- and bromo- carbynes (κ^3-Tp*). This means no complete isologous series differing only in the halogen is presently available, though

Table 2. Computationally Derived Data for [M(≡CX)L_2(Tp)] (M = Mo, W; X = F, Cl, Br, I; L = CO, Cl).[a]

X	M	L	Natural Charge			Löwden Bond Order		$r_{M\equiv C}$	ν_{CO}[b]	k_{CO}[c]	ν_{MC}	*TR*[d]
			M	C	X	M≡C	C–X	[Å]	[cm^{-1}]	Ncm^{-1}	[cm^{-1}]	
F	Mo	CO	+0.485	+0.276	–0.294	2.410	1.395	1.810	2023, 1962	16.04	1423	1.021
									(1995, 1935)	*15.60*		
Cl	Mo	CO	+0.614	–0.261	+0.074	2.472	1.334	1.794	2027, 1969	16.12	1153	1.033
									(1999, 1941)	*15.68*		
Br	Mo	CO	+0.624	–0.351	+0.143	2.495	1.267	1.790	2029, 1972	16.16	1110	1.037
									(2001, 1944)	*15.71*		
I	Mo	CO	+0.636	–0.480	+0.251	2.545	1.194	1.786	2030, 1975	16.20	1071	1.043
									(2002, 1947)	*15.75*		
Cl	W	CO	+0.945	–0.395	+0.064	2.450	1.315	1.809	2010, 1944	16.26	1179	1.030
									(1982, 1918)	*15.81*		
Cl	W	Cl	+1.474	–0.410	+0.065	2.671	1.318	1.767	–	–	1248	1.068

[a] DFT: ωBP97X-D/6-31G*/LANL2Dζ/gas phase. [b] Uncorrected values; Corrected values in parentheses. [c] Cotton-Kraihanzel force constant.[34] [d] ***TR*** = $2r(WN_{trans})/\Sigma r(WN_{cis})$.

Templeton has obtained [W(≡C-I)$(CO)_2$(Tp*)],[28] the only known iodocarbyne complex, via an alternative strategy.

To further explore their bonding, we also investigated a theoretical series of halocarbynes as ligands bound to a computationally pruned form of Lalor's archetypal halocarbyne complexes *viz.* [Mo(≡CX)$(CO)_2$(Tp)] (X = F, Cl, Br, I; Tp = hydrotris(pyrazolyl)borate, Figure 3), at the same level of computational cost (Table 2). The use of the reduced *tris*-pyrazolylborate ligand (Tp) as opposed to the real *tris*-(3,5-dimethylpyrazolyl)borate ligand (Tp*) was also used to reduce this cost further. The implications of this approximation upon derived data have been quantified in closely related systems and found to be acceptable.[32] Sadly, Lalor's halocarbyne synthesis in practice fails for this simpler borate.

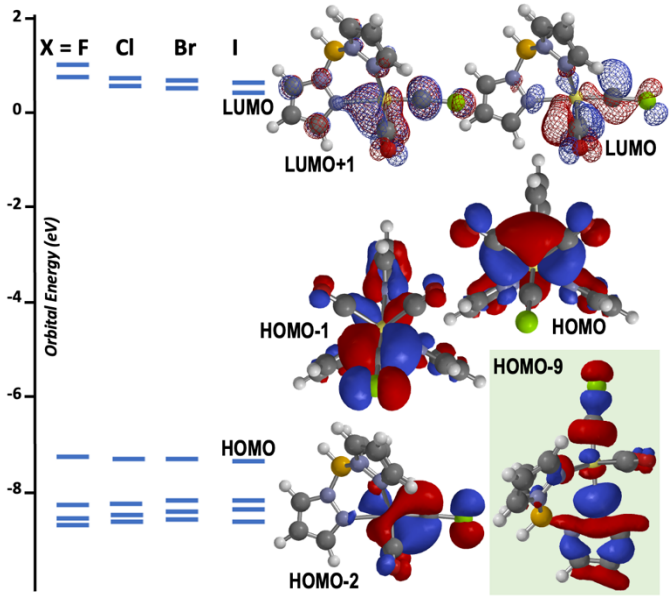

Figure 3. Frontier orbitals of interest for the halocarbyne complexes [Mo(≡CX)$(CO)_2$(Tp)] (X = F, Cl, Br, I; DFT: ωB97X-D/6-31G*/LANL2Dζ). The topologies for X = Cl (Isovalue = 0.032 √(e/au³)) are shown. Inset = HOMO-9.

As with other carbyne complexes of the form [M(≡CR)$(CO)_2$(Tp)] (M = Mo, W) for which computational data are available,[32,33] the HOMOs of [Mo(≡CX)$(CO)_2$(Tp)] are primarily associated with metal-carbonyl retrodonation. Being orthogonal to the M–CR vector, variations in the nature of 'R' do not impact significantly beyond what may be surmised experimentally from infrared data.[1e] The energy of this HOMO is accordingly invariant down the series. The HOMO-1 and HOMO-2 constitute the π-components of the Mo≡C bond. These are near to degenerate as would be expected given the axial symmetry of the halocarbyne ligand and the near degeneracy of the two t_{2g}-type retrodative orbitals of the 'Tp$(CO)_2$Mo' fragment. It should however be noted that this is not always the case; carbyne ligands of lower symmetry may result in these two orbitals being quite different in energy.[33a] The LUMO and LUMO+1 pair involve constructive π-overlap between the molybdenum and carbonyl ligands in combination with π*-antibonding Mo≡C character. This would seem consistent with the ambidentate electrophilicity demonstrated in reactions of [M(≡CR)$(CO)_2$(L)] (L = Tp, Tp*) carbyne complexes. There are numerous examples of halocarbynes and to a lesser extent thiolatocarbynes undergoing nucleophilic substitution at the carbyne carbon. There are, however, also cases where the carbonyl co-ligands provide an alternative site for nucleophiles to attack, *e.g.*, the kinetic product of the reaction of [W(≡CPPh_3)$(CO)_2$(Tp*)]$^+$ with Li[Et_3BH] is suggested to be the thermolabile formyl complex [W(≡CPPh_3){C(=O)H}(CO)(Tp*)].[28a]

Table 2 collates data arising from the computational studies and whilst the absolute values are prone to the particular foibles of the method of choice, we may assume within the narrow series of compounds considered that trends are reliably determined. From these data a number of features may be noted. With increasingly heavier halogen atoms, the Mo≡C bond order increases while the C-halogen bond order decreases. This is as would be expected from the decrease in effective pπ-pπ overlap between carbon and the increasingly diffuse halogen orbitals and increase in C–X bond length. This increase in Mo≡C bond order is also implicit in the gradual shortening of the metal-carbon bond from 1.810 to 1.786 Å. This fairly modest contraction is perhaps unlikely to be experimentally confirmed as it approaches the general limits of precision currently achieved through X-ray crystallography.

In terms of calculated natural charges, the fluorocarbyne is an outlier due to the exceptionally high electronegativity of fluorine

relative to the other halogens; the strong negative inductive effect (***I***$^-$) is not well-compensated by positive mesomeric stabilisation (***M***$^+$). Thus the fluorine in the fluorocarbyne carries a significant negative charge while the charge on the halogen in the remaining examples increases from near neutral (X = Cl) to *ca* +0.25 for X = I. The charge on the carbyne carbon for X = F is positive while for the remaining examples it is negative and increases from –0.26 (X = Cl) to –0.48 for X = I. The nett effect of the CX acceptor ligand on the charge on the molybdenum increases with the heavier halogen. This increased charge would be expected to be manifest in reduced retrodative capability and this is reflected by infrared data for the carbonyl co-ligands. Table 2 presents both the uncorrected ν_{CO} frequencies in addition to corrected values. Calculated vibrational frequencies are generally higher than experimentally determined values due to neglect of anharmonicity, incomplete incorporation of electron correlation and the use of finite basis sets.[35] The development of generic scaling factors (λ) assumes this over-estimation is relatively uniform. These λ-factors are however derived *via* least-squares analysis of calculated *vs* experimental frequencies for various test sets of molecules. Th test sets (i) in most cases involve first and second row elements but very rarely include metals and (ii) do not include fundamentals in our region of interest (1800 – 2200 cm^{-1}). Schlegel has, for example, provided distinct scaling factors for high (> 1800 cm^{-1}) and low-frequency (< 1800 cm^{-1}) infrared regions[36] while others have set the high/low boundary variously from 2500-2700 cm^{-1}.[37] In the absence of any known Tp-ligated halocarbyne complexes, the closest analogue to the model compounds would be [Mo(≡CCl)(CO)$_2${B(pz)$_4$}][13a] (cyclohexane: ν_{CO} = 2010, 1926 cm^{-1}). It is reasonable to assume that the hydrogen/pyrazolyl substitution is sufficiently remote from the metal so as to not have any significant electronic impact. The scaling factor implemented in *SPARTAN20®* (λ = 0.9400, provides lower frequencies than those derived using the scaling factor (λ = 0.9845) recommended for the ωBP97X-D/6-31G* combination.[38] This would therefore still appear to over-estimate the fundamental frequencies. Based on experimental data for [Mo(≡CCl)(CO)$_2${B(pz)$_4$}] and computational data for [Mo(≡CCl)(CO)$_2$(Tp)] we therefore suggest that a scaling factor of λ = 0.9266 is appropriate for these and related carbyne complexes and the resulting values are given in parentheses in Table 2.

Frequency calculations are performed to ensure that the derived geometries represent local energetic minima but they also provide an opportunity to identify the vibrational mode that *primarily* corresponds to the Mo≡C stretch. There is a gradual decrease in the frequency of the $\nu_{Mo\equiv C}$ mode proceeding from X = Cl (1153 cm^{-1}) to X = I (1071 cm^{-1}). This is perhaps counter-intuitive given the increase in Mo≡C bond order. More notably, however is what appears to be an anomalously high value for the fluorocarbyne (1423 cm^{-1}). Given that matrix-isolated difluoroethyne has a ν_{CF} value of 1346.9 cm^{-1},[39] we attribute this high value to the operation of Fermi resonance between the $\nu_{Mo\equiv C}$ and ν_{CF} modes. The substantially higher masses of the heavier halogens means that the corresponding ν_{CX} modes are too low in energy for effective mixing.

The comparatively high positive charge on iodine in [Mo(≡C-I)(CO)$_2$(Tp)] (I: +0.251) led us to consider the possibility that the iodide substituent might present a directional σ-hole for halogen bonding.[40] Figure 4 depicts the local electrostatic potential surface for [Mo(≡C-I)(CO)$_2$(Tp)] alongside those for iodoethyne (I: +0.339) and cyanogen iodide (I: +0.354) at the same level of theory, suggesting that this is indeed the case, though the effect is less pronounced than for either iodoalkynes or cyanogen iodide. Furthermore, the LUMO map for [Mo(≡C-I)(CO)$_2$(Tp)] (Figure 4d) indicates that in addition to coincidence with the σ-hole, the LUMO also has considerable contribution in the vicinity of the carbyne carbon, presenting an alternative competitive site for nucleophiles to approach. The sole examples[41] of iodocarbyne complexes [M(≡C-I)(CO)$_2$(Tp*)] (M = W **1e**, Mo **1f**) were described by Templeton from the reaction of [W(≡CLi)(CO)$_2$(Tp*)] with iodine[28b] and by Lalor from the reaction of [Et$_4$N][Mo(CO)$_3$(Tp*)] with [Ph$_3$S]BF$_4$ in iodoform in low yield.[13a] Accordingly, the subsequent chemistry of these unique species remains to be explored, although the corresponding *bromo*carbyne [Mo(≡CBr)(CO)$_2$(Tp*)] (**1d**) reacts with potential halogen bond acceptors *N,N*-dimethylaminopyridine and *N*-trimethylsilylimidazole *via* halide substitution rather than σ-hole coordination.[42]

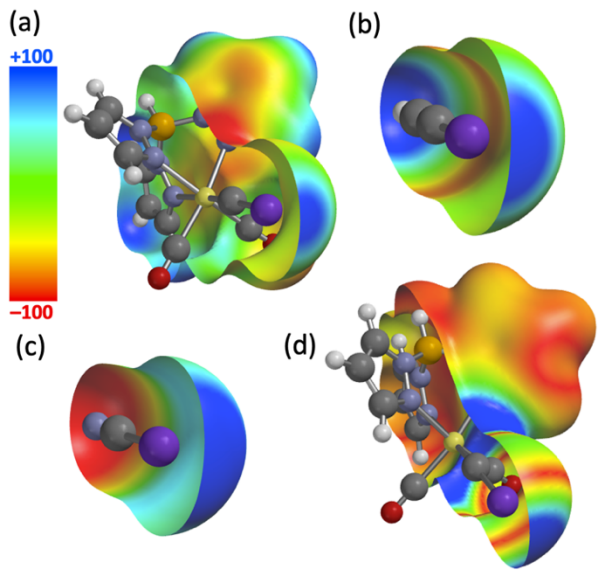

Figure 4. Electrostatic potential maps for (a) [Mo(≡C-I)(CO)$_2$(Tp)] (b) HC≡CI and (c) N≡C–I (DFT: ωB97X-D/6-31G*/LANL2Dζ; 0.002 e/au^3 isosurface) and (d) The LUMO map for [Mo(≡C-I)(CO)$_2$(Tp)].

The isolobal analogy[43] between C≡C and M≡C bonds inspired Stone to develop an extensive chemistry based on the coordination of mononuclear carbynes to extraneous metal centres.[44] Within this paradigm, the HOMO-1 and LUMO of carbyne complexes such as [Mo(≡CCl)(CO)$_2$(Tp)] (Figure 5) maps onto the frontier orbitals of ethyne. Acordingly, appending extraneous metal-ligand fragments to the triple bond allows a dimetallacyclopropene description to be considered akin to the Dewar-Chatt-Duncanson model of alkene coordination.[45]

Lalor's original report[6a] of the halocarbynes [M(≡CX)(CO)$_2$(Tp*)] (M = Mo, W; X = Cl, Br) immediately recognised their synthetic potential with respect to nucleophilic substitution. In the interim, Lalor,[6a,13,46] Templeton[47] Weber[8] and ourselves[9] have extensively exploited this reactivity but have also encountered failures with some nucleophiles. One method to overcome these problems has involved the use of cross-coupling protocols mediated by [Pd(PPh$_3$)$_4$]. In such processes, the bromocarbyne serves as the *C*-electrophile partner in combination with a range of nucleophiles. Alternatively,

conversion of the halocarbyne to the stannyl derivatives [M(≡CSnR$_3$)(CO)$_2$(Tp*)] (M = Mo, W; R = Me, ^{n}Bu)[48] allows the carbyne to serve the *C*-nucleophile role. Implicit in the former strategy is the intermediacy of heterobimetallic μ-carbido complexes of the form [MPd(μ$_2$-C)Br(CO)$_2$(PPh$_3$)$_2$(Tp*)]. Examples of these m-carbido complexes have more recently been isolated and structurally characterised.[23b] Beck had previously isolated one such complex [WPt(μ$_2$-C)Br(CO)$_2$(PPh$_3$)$_2$(Tp*)] in addition to an intermediate formulated as the μ-bromocarbyne complex [WPt(μ$_2$-CBr)(CO)$_2$(PPh$_3$)$_2$(Tp*)].[26a] Accordingly, there follows a range of attempts to isolate and fully characterise μ$_2$-halocarbyne complexes.

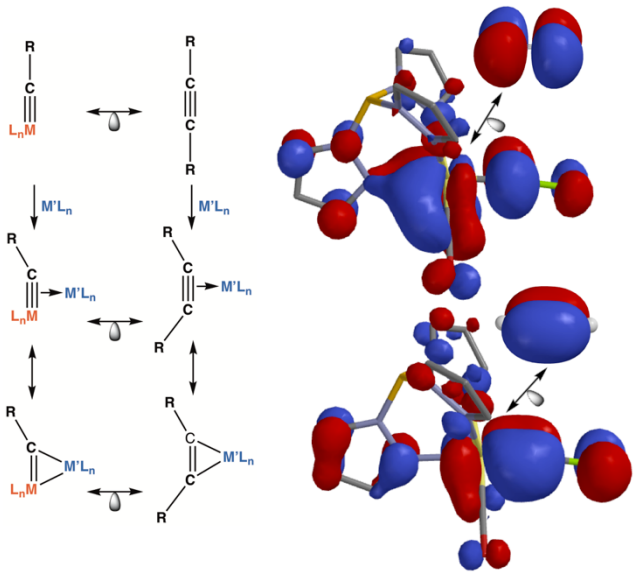

Figure 5. The Stone Paradigm: Isolobal mapping of CC and MC triple bonds with respect to dimetallacyclopropene formation. Frontier orbitals of ethyne *cf.* HOMO-1 and LUMO of [Mo(≡CCl)(CO)$_2$(Tp)].

Gold Bimetallic Halocarbynes

Given the slow but spontaneous conversion of [WPt(μ$_2$-CBr)(CO)$_2$(PPh$_3$)$_2$(Tp*)] into [WPt(μ$_2$-C)Br(CO)$_2$(PPh$_3$)$_2$(Tp*)] *via* insertion of platinum(0) into the C–Br bond, we first considered a metal less prone to oxidative addition, *viz.* gold(I). The coordination of metal-carbon multiple bonds to gold halides is well established both for carbene[49] and carbyne[50] ligands. Accordingly, the chlorocarbynes [M(≡CCl)(CO)$_2$(Tp*)] (M = Mo **1a**, W **1b**) were treated with [AuCl(SMe$_2$)] in dichloromethane, with precautionary exclusion of light, resulting in each case in a gradual colour change from bright yellow to orange over 30 minutes (Scheme 1). The reactions were accompanied by an increase in the values of ν_{CO} infrared absorptions. Attempts to purify the resulting complexes by anaerobic flash chromatography using silica gel or basic alumina resulted in rapid deposition of colloidal gold and diminished yields. Chromatography using diatomaceous earth followed by crystallisation, however afforded acceptable yields of pure materials as bright orange

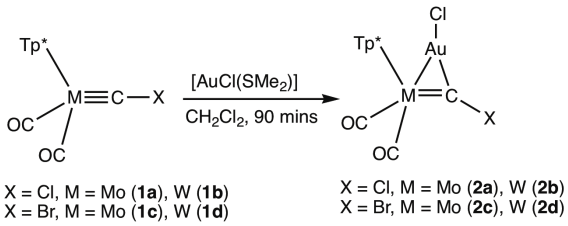

Scheme 1: Preparation of bimetallic gold halocarbyne complexes.

powders, formulated as the μ$_2$-chlorocarbynes [MAu(μ$_2$–CCl)Cl(CO)$_2$(Tp*)] (M = Mo **2a**, W **2b**).

In a similar manner and under the same conditions, the bromocarbynes [M(≡CBr)(CO)$_2$(Tp*)] (M = Mo **1c**, W **1d**) afforded bright orange μ$_2$-bromocarbyne complexes [MAu(μ$_2$-CBr)Cl-(CO)$_2$(Tp*)] (M = Mo **2c**, W **2d**). In each case, coordination of the 'AuCl' fragment to the carbyne resulted in a rather small shift in the associated ^{13}C resonances (δ_C: 212.1–230.4) relative to the precursors **1a-d** (δ_C: 198.0–208.7). In general, far more pronounced shifts to high frequency are associated with conversion of terminal carbyne to μ$_2$-coordination, however this tends to a be a recurrent characteristic feature of aurometallacyclopropenes. Appending the AuCl units results in a reduction of the π-basicity of the molybdenum or tungsten centres, as reflected by increases in the ν_{CO} values for the carbonyl ligands.

The molecular structures of **2a–2d** were all confirmed by diffraction studies that confirmed the formulations that followed from spectroscopic studies. The molecular geometries of two examples, **2a** and **2d**, are presented in Figures 6 and 7, respectively.

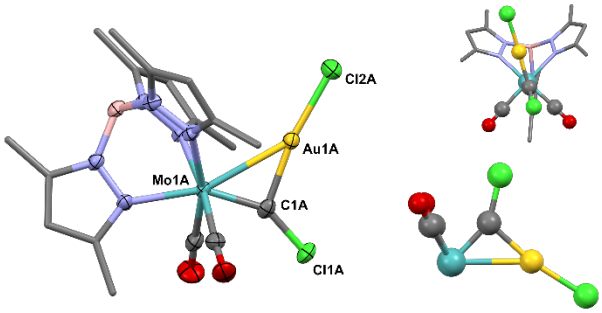

Figure 6: Molecular structure of **2a** in a crystal (50% displacement ellipsoids, pyrazolyl ligands simplified and hydrogen atoms omitted, one of two crystallographically independent molecules shown). Insets = View along the Mo–C axis and a simplified model to highlight the deviation of the chlorocarbyne ligand about the two metallic centres.

Geometric data of interest are collated in Table 3 alongside those calculated for the simplified complex [MoAu(μ$_2$-CBr)Cl(CO)$_2$(Tp)] (**2'**, DFT: ωB97X-D/6-31G*/LANL2Dζ). With the exception of the over-estimated metal-metal bond length, the remaining bond lengths and angles are similar to the experimentally deteremined mean values, which themselves span remarkable small ranges for the seven molecules. It is quite appropriate to consider the molybdenum and tungsten examples collectively because for all practical intents and purposes we may consider the *4d* and *5d* members of group 6 to have essentially the same covalent radii.

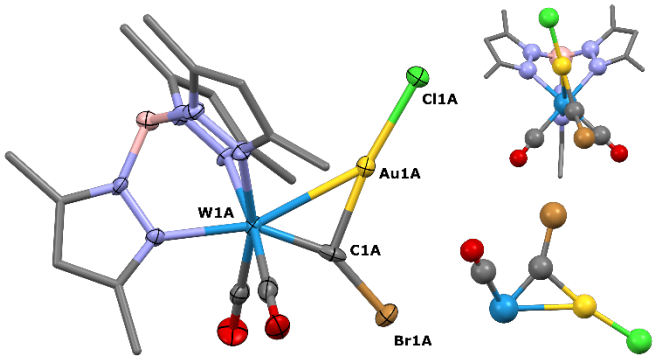

Figure 7: Molecular structure of **2d** in a crystal (50% displacement ellipsoids, pyrazolyl ligands simplified and hydrogen atoms omitted, one of two crystallographically independent molecules shown). Insets = View along the W–C axis and a simplified model to highlight the deviation of the bromocarbyne ligand about the two metallic centres.

Statistical harvesting of the CCDC empirically suggests the covalent radius for tungsten (1.62 Å) is larger than that for molybdenum (1.54 Å)[51] whilst Pykkö's analysis of triple-bond covalent radii[52] affords more similar values for tungsten (1.15 Å) and molybdenum (1.13 Å). For double bonds similar treatment also affords more similar values (W: 1.20 Å; Mo 1.21 Å).[53] It should, however, be appreciated that the former approach carries a statistical bias associated with the classes of compound selected for crystallographic studies. Neither approach adequately addresses the variation in covalent radius with coordination number.

Table 3. Structural data for μ-halocarbyne complexes of gold [MAu(μ_2-CX)Cl(CO)$_2$(Tp*)] (M = Mo, W; X = Cl, Br)

M	X		M=C [Å]	M–Au [Å]	Au–C [Å]	M–C–X [°]	Au–C–X [°]
Mo	Cl	**2a**[a]	1.879(7)	2.7778(6)	2.021(8)	149.4(5)	119.7(4)
			1.892(7)	2.7700(6)	2.014(7)	149.4(4)	120.3(4)
W	Cl	**2b**	1.892(6)	2.7926(3)	2.025(5)	148.9(3)	120.2(3)
Mo	Br	**2c**[a]	1.887(9)	2.7830(7)	2.038(9)	151.5(5)	118.2(4)
			1.887(7)	2.7763(7)	2.010(9)	149.6(5)	119.6(4)
W	Br	**2d**[a]	1.893(17)	2.771(1)	2.057(18)	152.7(11)	118.2(9)
			1.885(19)	2.7780(11)	2.029(17)	150.3(10)	119.2(9)
Mean:			*1.888*	*2.778*	*2.028*	*150.3*	*119.3*
Mo	Br	**2'**[b]	1.888	2.833	2.037	147.8	119.8

[a]Two crystallographically independent molecules. [b]Calculated for [MoAu(μ-CBr)Cl(CO)$_2$(Tp)], DFT: ωB97X-D/6-31G*/LANL2Dζ/gas phase

Taking the structural models together along with the considerable body of data available for carbynes bridging gold to tungsten and to a lesser extent molybdenum[1e,50b-g] (no chromium examples have been investigated), geometric features peculiar to gold coordination emerge. The Mo–C and W–C bond lengths (1.879-1.893 Å) are not significantly elongated relative to the corresponding bond lengths for the terminal halocarbynes **1c**, **1g** and **1h** (1.798-1.910 Å). From a Dewar-Chatt-Duncanson-type perspective of the M≡C triple bond coordinating to the gold(I) centre, the minimal impact on this bond length might be taken to indicate that π-retrodonation from d^{10}-Au(I) to one π* orbital of the M≡C triple bond is rather modest. This is manifest in only a comparatively small contraction of the M–C–X (X = Cl, Br) angles, which all fall within the narrow range of 149.4–152.6°. The homometallic halocarbyne complexes [Rh$_2$(μ_2-CX)(μ_2-X)X$_4$(dppm)$_2$] (X = Cl, Br),[22] in which the halocarbyne ligand coordinates *symmetrically* to two rhodium centres have Rh–C–X angles of 123.6°, 125.1° (X = Cl) and 129.9° (X = Br), *i.e.*, near to the ideal value for an sp^2-hybridised carbon.

Stone has discussed the unsymmetrical geometry of μ-carbynes bridging metal-gold bonds in the context of the carbaborane complex [WAu(μ_2-CC$_6$H$_4$Me-4)(CO)$_2$(PPh$_3$)(η^5-C$_2$B$_9$H$_{11}$Me$_2$)].[46c,54] He concluded that it might be described as a 'semi-bridging' carbyne (Chart 2b) ligand rather than the dimetallacyclopropene description (Chart 2a) that is more apt for less disparate metals.

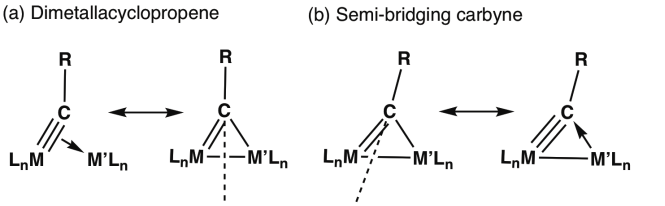

Chart 2. Dimetallacyclopropene vs semi-bridging geometries for bridging carbyne ligands.

Thus as with carbonyl ligands,[55] semi-bridging character arises when the ligand whilst essentially terminally bound to one metal, is nevertheless able to withdraw electron density from a second metal in what we might now term a Z-type (Lewis acidic) or polar-covalent interaction.[56] This interpretation has arisen from a consideration of geometric features, however with computational results in hand for **2'** (Figure 8) we are now in a position to explore this description.

Firstly, it may be recalled that the calculated bond order for the MoC bond of [Mo(≡CBr)(CO)$_2$(Tp)] was 2.495 (*vide supra*), consistent with its description as an essentially triple bond, somewhat diminished by pπ(C)- pπ(Br) overlap. At the same level of theory, the bond order for **2'** is found to be 1.829, with the lost bonding to carbon and molybdenum being taken up by the Mo–Au (LBO = 0.659 and Au–C (LBO = 0.849) interactions. The natural negative charge on the bridging carbyne carbon (–0.895) is increased markedly from –0.351 in the mononuclear terminal carbyne [Mo(≡CBr)(CO)$_2$(Tp)] while the positive charge on molybdenum (+0.577) is only slightly decreased (from +0.624). Relative to charges on gold calculated for the hypothetical Cl–Au (+0.701) and Cl–Au(η^2-HCCH) (+0.990) molecules, the charge on gold (+1.067) in **2'** points to a net flow of electron density from gold to molybdenum and carbon atoms. These observations suggest that both the dimetallacyclopropene and semi-bridging carbyne canonical descriptions (Chart 2) serve a purpose in describing the bonding. Inspection of the molecular orbitals of **2'** (Figure 8) also indicates that no single two-centre, two-electron bonding interaction description entirely accounts for the μ-carbyne bonding. Within the AuCMo moiety a number of interactions of both σ and π symmetry with respect to the Au-C vector are of note. Deep within the manifold, the HOMO-22 most closely resembles the semi-bridging Au→C interaction. The HOMO-21, however, involves an interaction that is both Au–C and C–Br π-bonding in nature. The HOMO-16 contributes to both Au–Mo and Au–C σ-bonding while the HOMO-3 reflects the retention of Mo-C π-bonding orthogonal to the MoCAu plane. By employing a labile source of 'AuCl', terminal halocarbynes have provided entry into μ_2-halocarbynes in one step. Perhaps the most valuable development is not the realisation of rare species, but that the bimetallic halocarbynes retain intact C–Cl or C–

Br for further functionalisation. In this respect, it should be noted that the LUMO+1 of **2'** includes a substantial contribution from the carbyne p orbital orthogonal to the MoCAu plane.

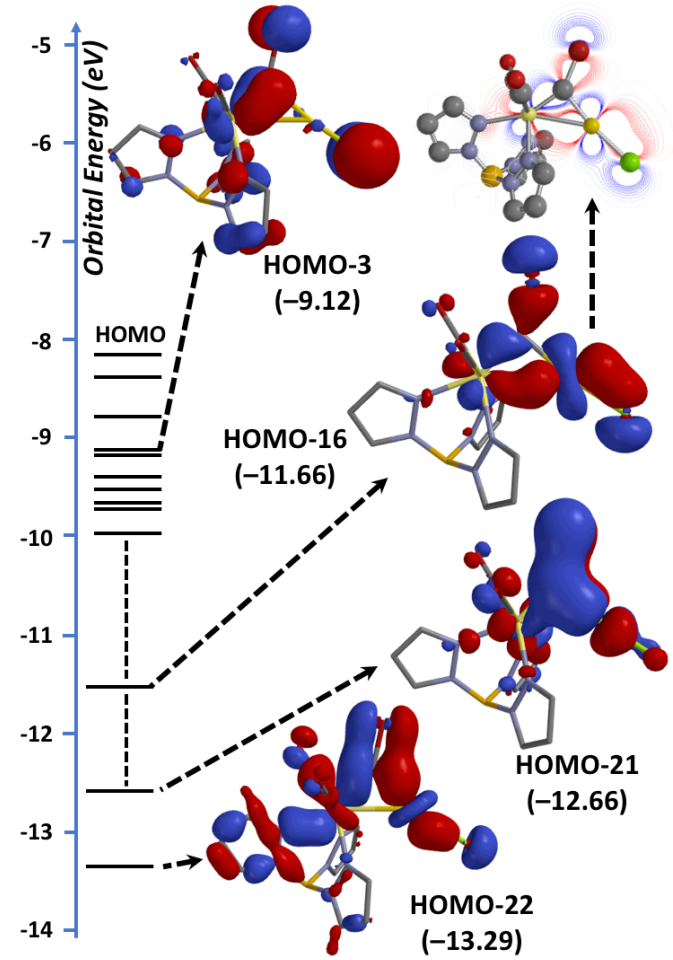

Figure 8. Molecular orbitals of interest for the gold μ-bromocarbyne complex [MoAu(μ_2-CBr)Cl(CO)$_2$(Tp)] (**2'**: DFT: ωB97X-D/6-31G*/LANL2Dζ, Isovalue = 0.032 √(e/au^3)).

Platinum Bimetallic Halocarbynes

Given the spectroscopic observation of a μ_2-bromocarbyne complex [WPt(μ_2-CBr)(CO)$_2$(PPh$_3$)$_2$(Tp*)] (**3c**), *en route* via oxidative addition to the heterobimetallic carbido complex [WPt(μ_2-C)Br(CO)$_2$(PPh$_3$)$_2$(Tp*)],[23] we sought further cases where platinum(0) interacts with the multiple bond of halocarbynes without, or prior to, insertion into the C–halogen bond, encouraged by the isolation of **2a-d**. In our own studies of platinum carbido complexes[23b] we have so far failed to secure crystals of **3c** suitable for crystallographic analysis, but reasoned that since C-Cl bonds are generally less reactive than C–Br bonds with respect to oxidative addition, platinum μ-chlorocarbyne complexes might be arrested, where μ-bromocarbynes are not. To discourage C–Cl bond polarisation that might encourage oxidative addition (*vide infra*), THF (κ = 7.52) rather than polar CH_2Cl_2 (κ = 9.08) was employed in reactions of terminal halocarbynes with [Pt(η^2-CH$_2$=CH$_2$)(PPh$_3$)$_2$]. Stirring halocarbynes **1a** or **1b** in THF at room temperature with [Pt(η^2-CH$_2$=CH$_2$)(PPh$_3$)$_2$] resulted in a slow colour change from yellow to dark orange over several hours, as monitored by *in situ* infra-red spectroscopy. If the reaction mixture is heated under reflux, conversion to the new products is complete within 30 minutes, though prolonged heating should be avoided (*vide infra*).

Although ^{31}P{^{1}H} NMR spectroscopy of the crude product indicated essentially quantitative conversion to the new μ_2-chlorocarbyne complexes [MPt(μ_2-CCl)(CO)$_2$(PPh$_3$)$_2$(Tp*)] (M = Mo **3a**; W **3b**, Scheme 2, Tables 4 and 5), isolation of pure materials proved non-trivial. Attempts to purify either **3a** or **3b** by flash chromatography (alumina or silica gel) resulted in isomerisation to a new compound (*vide infra*). For this reason, crystallisation by dilution with *n*-hexane and concentration under reduced pressure afforded olive-yellow solids identified as pure **3a** or **3b**.

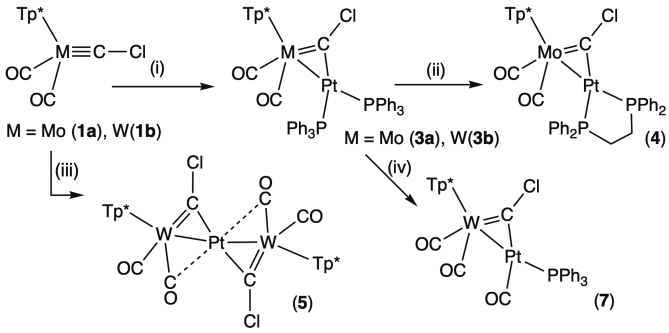

Scheme 2: Preparation of Platinum chlorocarbynes. (i) [Pt(η^2-C$_2$H$_4$)(PPh$_3$)$_2$], Δ, THF. (ii) dppe, THF, r.t. (iii) [Pt(nbe)$_3$], THF, r.t. (iv) CO, r.t.

Table 4. Structural data for μ-chlorocarbyne complexes of platinum [MPt(μ_2-CCl)(CO)$_2$(L)$_2$(Tp*)] (M = Mo, W; L = PPh$_3$, ½ dppe, PMe$_3$, CO)

M	L		M=C [Å]	M–Pt [Å]	Pt–C [Å]	M–C–X [°]	Pt–C–X [°]
Mo	PPh$_3$	**3a**[a]	1.934(5)	2.7913(4)	1.986(4)	135.8(3)	133.4(3)
			1.955(4)	2.7999(4)	1.958(5)	134.1(3)	134.5(3)
W	PPh$_3$	**3b**[a]	1.952(7)	2.7961(4)	1.988(6)	136.3(4)	133.3(4)
			1.970(7)	2.8078(4)	1.964(6)	134.2(4)	134.7(4)
Mo	½ dppe	**4**[a]	1.937(4)	2.7618(3)	2.086(4)	142.8(3)	130.0(2)
W	CO/PMe$_3$	7	1.951(4)	2.7732(2)	1.950(4)	136.2(2)	133.2(2)
Mean:			1.950	2.791	1.996	136.6	133.2
Mo[b]	*PMe$_3$*	***3'^{Mo}***	*1.934*	*2.816*	*1.950*	*133.1*	*133.9*
Mo[b]	*CO/PMe$_3$*	***7'^{Mo}***	*1.917*	*2.818*	*1.991*	*137.6*	*130.0*
W[b]	*PMe$_3$*	***3'^{W}***	*1.940*	*2.815*	*1.955*	*133.9*	*133.6*
W[b]	*CO/PMe$_3$*	***7'^{W}***	*1.926*	*2.815*	*1.990*	*138.4*	*129.5*

[a]Two crystallographically independent molecules. [b]Calculated for [MPt(μ_2-CCl)(CO)$_{4-n}$(PMe$_3$)$_n$(Tp)] (n = 1, 2), DFT: ωB97X-D/6-31G*/LANL2Dζ/gas phase

The most characteristic indication of the formation of **3a**/**3b** is manifest in the ^{31}P{^{1}H} NMR spectra, as a result of the coupling of multiple spin-active nuclei. With specific reference to species **3a** (**3b** is similar), two doublets are observed for an **AB** system with a small coupling ($^2J_{AB}$ = 24 Hz) consistent with the *cis* disposition of two chemically inequivalent phosphines. Furthermore, the coupling to ^{195}Pt (*I* = ½, 33% natural abundance) results in each doublet being straddled by satellites with strikingly different coupling constants, *i.e.*, the respective phosphines lie *pseudo-trans* to the Mo–Pt and C–Pt bonds with very disparate *trans* influences.

Table 5. Selected NMR data[a] for μ-chlorocarbyne complexes of platinum [MPt(μ_2-CCl)(CO)$_2$(PR$_3$)$_2$(Tp*)] (M = Mo, W; PR$_3$ = PPh$_3$, ½ dppe)

M	PR$_3$		δ_C [ppm]	$^2J_{PC}$ [Hz]	δ_P [ppm]	$^1J_{PtP}$ [Hz]	δ_{Pt} [ppm]
Mo	PPh$_3$	**3a**	314.8	73.9	38.2	4396	–3940
				7.0	25.8	2760	
W	PPh$_3$	**3b**	297.2	75.7	41.9	4317	–3992[c]
				5.3	24.4	2560	
Mo	½ dppe	**4**	324.2	73.9	48.2[b]	4023	–4203
				d	47.8[b]	2668	

[a]Measured in C$_6$D$_6$, 25 °C. [b]Not corrected for roofing. [c] $^1J_{WPt}$ = 370 Hz. [d] not resolved

As for **2a-2d**, but more dramatically, coordination of the M≡C bond to platinum results in a significant shift in the carbyne resonances in the $^{13}C\{^1H\}$ NMR spectra to higher frequency (δ_C = 314.1 for **3a** *cf.* 208.7 for **1a**). The $^{195}Pt\{^1H\}$ resonance is consistent with platinum(0)[57] (δ_{Pt} = –3940) and also more conventional carbyne complexes of the type [MPt(μ_2-CR)(CO)$_2$(PR'$_3$)$_2$(Tp)] (M = Mo, W; R = Me, C$_6$H$_4$Me-4; R' = Me, OMe).[24d] With the exception of **3c**, complexes of this form have not been reported for the bulkier Tp* and PPh$_3$ co-ligand combination.

Large red/orange plates of both **3a** and **3b** acetonitrile solvates were obtained *via* solvent vapour diffusion for crystallographic analysis, the results of which are summarised in Figures 9 and 10, respectively. With the two structures being isomorphous, only **3a** need be discussed in detail.

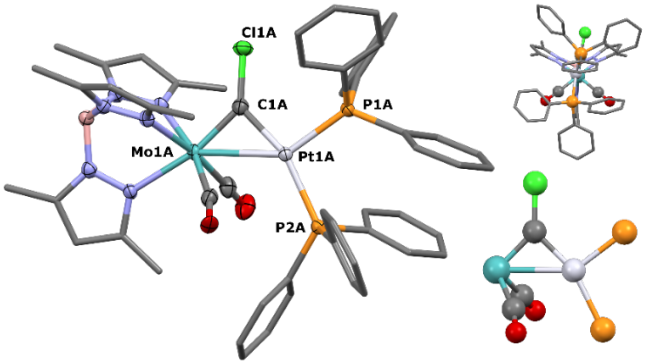

Figure 9: Molecular structure of **3a** in a crystal 2(**3a**)·2.5(MeCN) (50% displacement ellipsoids, pyrazolyl and phenyl rings simplified with hydrogen atoms omitted for clarity, one of two crystallographically independent molecules shown). Insets = View along the W–Pt axis and a simplified model to highlight the symmetry of the chlorocarbyne ligand about the two metallic centres.

Taking the 'Mo≡C' unit as a single ligand, the geometry may be described as involving *pseudo*-trigonal planar platinum(0) with the Mo≡C bond lying in the coordination plane, *cf. e.g.*, the dichloroethyne ligand in [Pt(η^2-ClCCCl)(PPh$_3$)$_2$],[58] a complex with a number of parallels with **3a,b**, from both isolobal and reactivity perspectives, not least its thermal rearrangement to the chloroalkynyl complex [Pt(C≡CCl)Cl(PPh$_3$)$_2$] (*vide infra*). Within the Dewar-Chatt-Duncanson paradigm, the geometry could also be considered as a d^8-square planar platinacyclopropene, the geometric constraints of *dihapto* coordination notwithstanding. Similar arguments apply to 'Pt(PR$_3$)$_2$' adducts of more conventional carbyne complexes, *e.g.*, [WPt(μ_2-CC$_6$H$_4$Me-4)(CO)$_2$(PMe$_2$Ph)$_2$(η-C$_5$H$_5$)].[24a,f] For both **3a** and **3b**, the Pt–P1A bond lengths were significantly contracted when compared to Pt–P2A distances, which in part explains the dramatic difference between the $^1J_{PtP}$ couplings, *e.g.*, 4398 and 2761 Hz for **3a**.

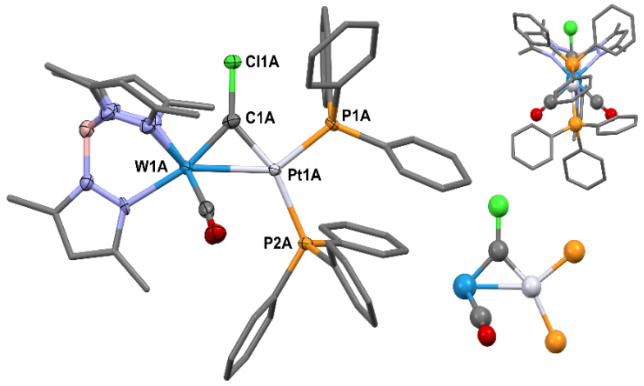

Figure 10: Molecular structure of **3b** in a crystal of **3b**·3(MeCN) (50% displacement ellipsoids, pyrazolyl and phenyl rings simplified with hydrogen atoms omitted for clarity). Insets = View along the W–Pt axis and a simplified model to highlight the symmetry of the chlorocarbyne ligand about the two metallic centres.

The 'Pt(PPh$_3$)$_2$' unit is seen to add *syn* to the carbonyls rather than *anti* as in the case of **2a-d**, allowing the sterically obtrusive PPh$_3$ ligands to avoid unfavourable inter-ligand repulsion with the dimethylpyrazolyl groups. The W–Pt bond lengths in **3b** (2.7961(4), 2.8078(4) Å) are significantly different (29 e.s.d.) and marginally longer than the W–Au bond in **2b** (2.7926(3) Å) despite gold and platinum being considered to have similar covalent radii (1.36 Å).[53] More noticeable, however, is that the chlorocarbyne bridge M–C1A–Cl1A angle is contracted for both **3a** (135.9(3)°) and **3b** (134.3(4)° relative to that for **2b** (148.9(3)°). Thus, while still having some semi-bridging character, the halocarbyne bridge is somewhat more symmetrically disposed between the group 6 metals and platinum. This may suggest that more retrodonation occurs from Pt(0) than Au(I) resulting in more *sp*^{2} character for the carbyne carbon. The caveat for this interpretation is that the platinum(0) is supported by two large PPh$_3$ ligands, however the structures do not appear to exhibit any significant inter-ligand repulsion issues, and we note a corresponding W–C–C angle of 137.9° for the less sterically encumbered complex [WPt(μ_2-CC$_6$H$_4$Me-4)(CO)$_2$(PMe$_2$Ph)$_2$(η-C$_5$H$_5$)].[24a,f] The W–C–Cl angles in **3a,b** *cf.* **2a,b** would therefore appear to be genuine responses to electronic factors rather than steric impacts. This is also consistent with the geometry and molecular orbitals derived for the sterically less encumbered hypothetical model [MoPt(μ_2-CCl)(CO)$_2$(PMe$_3$)$_2$(Tp)] (**3'**, Figure 12) which has a Mo–C–Cl angle of 133.1 with Mo–C and Mo–Pt bond lengths of 1.934 and 2.816 Å, respectively.

The frontier orbitals of interest for **3'** presented in Figure 11 include the LUMO, which is localised on the chlorocarbyne carbon but also has contributions from molybdenum and one carbonyl ligand. The HOMO remains primarily associated with carbonyl retrodonation while the HOMO-1 corresponds to the remaining π-bonding of the chlorocarbyne to molybdenum and the HOMO-2 is in part associated with Mo–Pt σ-bonding.

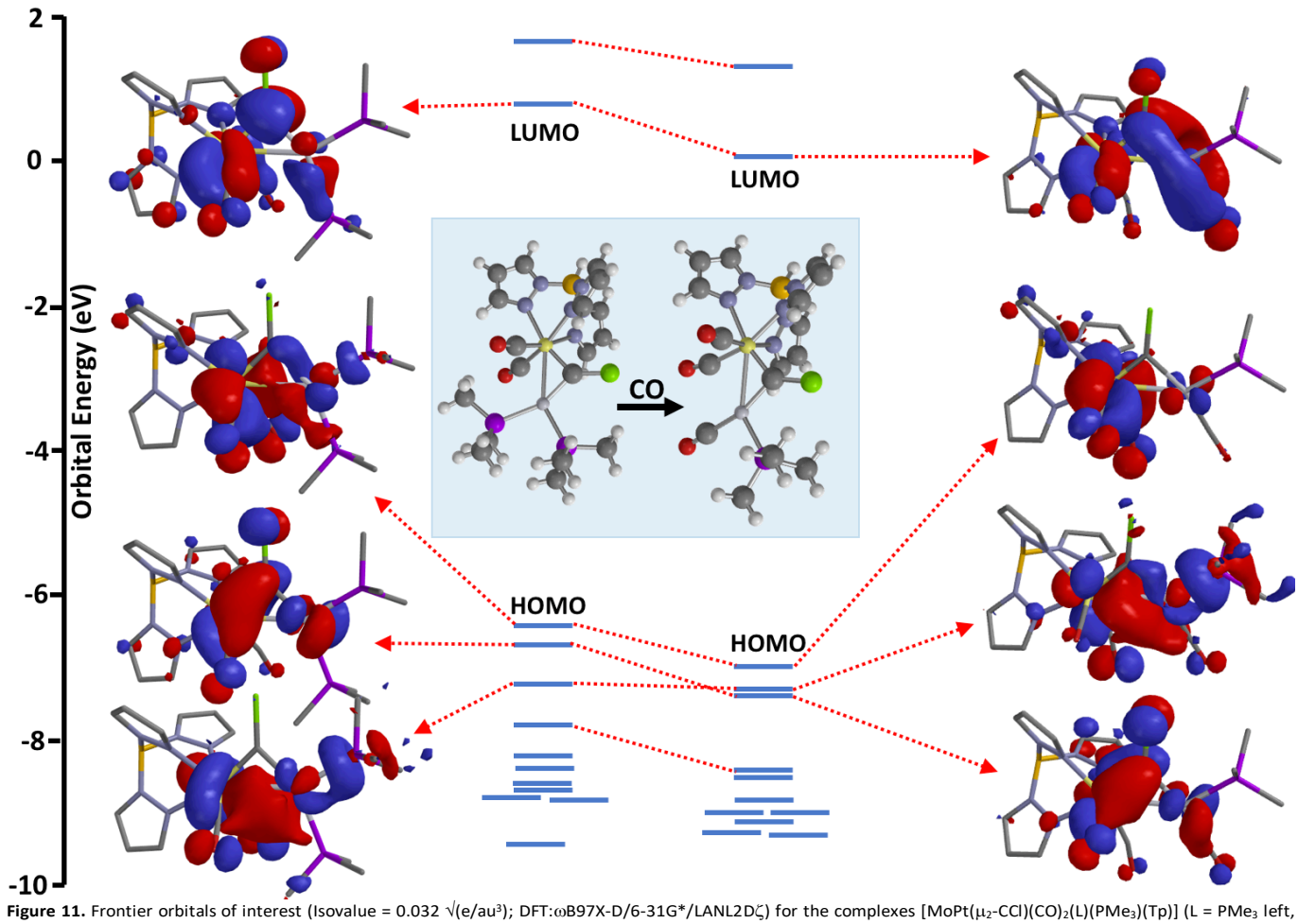

Figure 11. Frontier orbitals of interest (Isovalue = 0.032 √(e/au³); DFT:ωB97X-D/6-31G*/LANL2Dζ) for the complexes [MoPt(μ_2-CCl)(CO)$_2$(L)(PMe$_3$)(Tp)] (L = PMe$_3$ left, CO right). For orbital energies of [WPt(μ_2-CCl)(CO)$_2$(L)(PMe$_3$)(Tp)] see Figure S20 in ESI.

Given that μ_2-halocarbynes remain scarce, ligand substitution was investigated employing **3a**, which was found to react readily with the chelating phosphine 1,2-bis(diphenylphosphino)ethane (dppe), to afford the new chlorocarbyne [MoPt(μ_2-CCl)(CO)$_2$(dppe)(Tp*)] (**4**). The optimal conditions for the preparation of **4** involved successive treatment of **1a** with [Pt(η^2-H$_2$C=CH$_2$)(PPh$_3$)$_2$] and then dppe, without isolation of **3a** for reasons to be discussed below. Relative to **3a**, the chelated complex **4** is somewhat more stable and can be purified by flash chromatography.

Spectroscopic and crystallographic (Figure 12) analysis of **4** revealed features similar to **3a**, in addition to the presence of a semi-bridging carbonyl ligand that is evident in the solid state (Pt1···C3 = 2.364(4) Å, Mo1–C3–O2 = 157.0(8)°) and by infra-red spectroscopy in both solid and solution phases (ν_{CO} = 1772 cm^{-1}) but which does not endure on the ^{13}C NMR timescale (single MoCO resonance, δ_C = 230.7). The chelate bite of the dppe ligand results in a contraction of the P1-Pt1-P2 angle (86.58(3)°) relative to that in **2a** (100.60(4)°) however the same variation in platinum-phosphorus bond lengths is observed with that *pseudo-trans* to the carbyne carbon being elongated (2.2878(9) Å) relative to that *pseudo-trans* to the molybdenum (2.249(1) Å). Again, this is manifest in markedly differing values for the $^1J_{PtP}$ couplings (4030, 2671 Hz) for the chemically inequivalent phosphorus nuclei (δ_P = 48.2, 47.8).

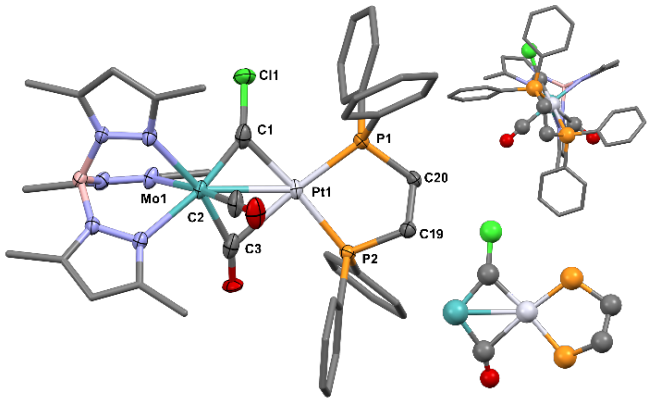

Figure 12. Molecular structure of **4** in a crystal (50% displacement ellipsoids, pyrazolyl and phenyl rings simplified with hydrogen atoms omitted for clarity, positional site exchange disorder between Cl1 and O2 sites). Selected bond lengths (Å) and angles (°): Mo1–C1 1.937(5), C1–Cl1 1.663(5), Pt1–C1 2.087(4), Mo1–Pt1 2.7618(4), Pt1–P1 2.249(1), Pt1–P2 2.2878(9), Mo1–C1–Cl1 142.8(3), Pt1–C1–Cl1 130.0(3), P1–Pt1–P2 86.58(3). Insets = View along the W–Pt axis and a simplified model to highlight the symmetry of the chlorocarbyne ligand about the two metallic centres.

The Mo1–C1 bond length (1.937(5) Å) is identical in length to that observed for **3a** (1.934(4) Å) although the Mo1–C1–Cl1 angle is somewhat wider at 142.8(3)° (*cf.* 135.9(3)° for **3a**) while the Mo1–Pt1 bond (2.7618(4) Å) is contracted relative to the other examples,

presumably because the chelation brings the two phosphine donors closer together to allow the molybdenum to more closely approach.

A Trimetallic Bis-Halocarbyne

Stone has previously described a series of 'bow-tie' trimetallic bis(μ-carbyne) complexes of the form $[M_2M'(\mu_2\text{-}CR)_2(CO)_4(L)_2]$ (M = Cr, Mo, W; R = Me, Ph, C_6H_4Me-4, ½ $Fe(C_5H_4)_2$; L= η^5-C_5H_5, η^5-C_5Me_5, κ^3-Tp; M' = Ni, Pd, Pt, Cu^+, Ag^+, Au^+, $Mo(CO)_2$, $W(CO)_2$)[24a,45a,59] to which we have recently added the parent bis(methylidyne) $[W_2Pt(\mu_2\text{-}CH)_2(CO)_4(Tp^*)_2]$.[60] Given the coordination of halocarbynes to zerovalent platinum demonstrated above, the challenge of preparing a similar bis(chlorocarbyne) 'bow-tie' was addressed. The reaction of **1b** with the 'ligand-free' platinum source $[Pt(nbe)_3]$[61] in THF immediately gave a yellow solution, which quickly darkened to orange and eventually red over 24 hours. The compound was found to successfully elute through a flash column and could be subsequently crystallised to give a bright red powder. Spectroscopic data were consistent with the formulation as a trimetallic bow-tie $[W_2Pt(\mu_2\text{-}CCl)_2(\mu\text{-}CO)_2(CO)_2(Tp^*)_2]$ (**5**, Scheme 2) which proved to be remarkably stable.

Whilst a crystallographic structure determination unambiguously confirmed the formulation, the precision of the structural model was compromised by disorder involving the platinum, CO and CCl units (Figure 13), although the connectivity is assured. The platinum atom was disordered about, but not on, a special position (inversion centre ½, 0, ½). Thus the sterically engulfing $(WTp^*)_2$ periphery which dominates crystal packing and could be adequately modelled, falsely imposes a crystallographic (almost D_{3d}) centrosymmetry on the central region of most interest. Figure 9 depicts the major disorder component but we eschew any analysis beyond visual inspection of the molecular topology.

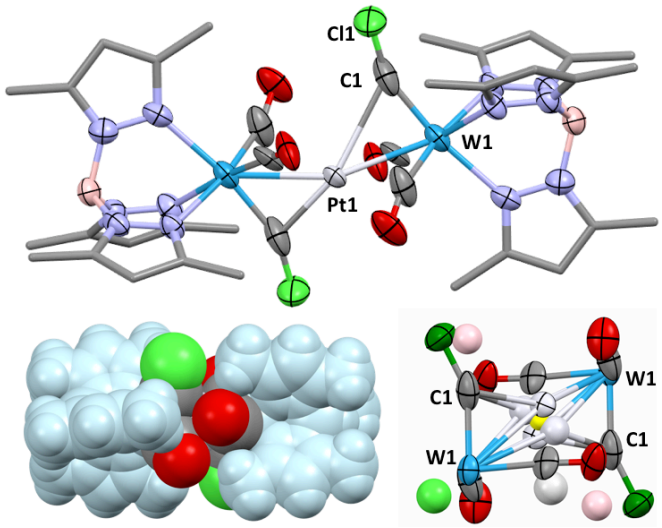

Figure 13. Molecular structure of **5** in a crystal (50% displacement ellipsoids, pyrazolyl rings simplified and hydrogen atoms omitted for clarity, major disorder components shown). The platinum atom is positionally disordered near to but not at an inversion centre. Insets = Space-filling representation of (blue) Tp*W caps surrounding disordered central collar and depiction of disorder associated with the $W_2Pt(CO)_4(CCl)_2$ core about the (yellow) inversion centre.

The ^1H NMR spectrum was found to be broadened at room temperature consistent with a dynamic system—a feature also apparent in the spectra of the analogous bis(methylidyne) species $[W_2Pt(\mu_2\text{-}CH)_2(CO)_4(Tp^*)_2]$.[60] Upon cooling to –30 °C the ^1H NMR spectrum sharpens and at –40 °C, with the fluxionality arrested, each individual resonance for the Tp* ligands could be identified due to the chiral C_2-symmetric ground-state structure rendering all of them chemically inequivalent. Similarly, $^{13}C\{^1H\}$ spectra measured at –40 °C, revealed the μ_2-chlorocarbyne resonance at δ_C = 267.9 to slightly higher field of the resonances observed for **3a,b** and **4**. The platinum NMR spectrum (150.2 MHz, 25 °C) comprises a broadened resonance (h.h.w. = 216 Hz) at δ_{Pt} = –2063, again reflecting the inferred fluxionality, and significantly more downfield than for **3a,b** or **4**. At –40°C, one carbonyl from each tungsten assumes a semi-bridging role (δ_C = 227.2) distinct from the terminal carbonyl ligands (δ_C = 219.2)

Isomerism of a μ_2-halocarbyne

During preparations of **3b**, a recurrent isomerism was observed which was accelerated by polar media such as flash chromatography through silica gel, or unpurified commercial grade $CDCl_3$. Smooth conversion of **3b** to an orange species was accompanied by new infra-red and $^{31}P\{^1H\}$ signals absent from spectra of the sample prior to chromatography. This new compound was identified as the μ_2-carbido complex $[WPt(\mu_2\text{-}C)Cl(PPh_3)_2(CO)_2(Tp^*)]$ (**6**). Beck has noted the thermally-induced conversion of $[MoPt(\mu_2\text{-}CBr)(PPh_3)_2(CO)_2(Tp^*)]$ to $[MoPt(\mu_2\text{-}C)Br(PPh_3)_2(CO)_2(Tp^*)]$ which required heating under reflux in benzene (*ca* 80°C, 1 h). In contrast, heating **3b** in d_8-toluene at 60 °C for 48 hours resulted in no discernible formation of **6**. When **3a** is heated in $CDCl_3$ that has been purified by distillation under dry argon and storage over silver wire and 3 Å molecular sieves, the half-life for this isomerism is *ca* 960 min at 60 °C. When, however 'benchtop' $CDCl_3$ is used, as received, the reaction is noticeably accelerated and complete within 48 hours. Takao has also recently observed the conversion of $[Ru_2(\mu_2\text{-}CCl)(\mu\text{-}Cl)Cl_2(\eta\text{-}C_5Me_5)_2]$ to a dimetallacumulenic carbido complex $[Ru_2Zn(\mu_2\text{-}C)Cl_2(\mu_3\text{-}dmm)_2(\eta\text{-}C_5Me_5)_2]$ (dmm = dimethylmaleate) upon reduction with zinc in the presence of dmm. The same but spontaneous conversion in polar solvents (*e.g.,* CH_2Cl_2) therefore calls for comment and suggests an alternative mechanism (Scheme 3).

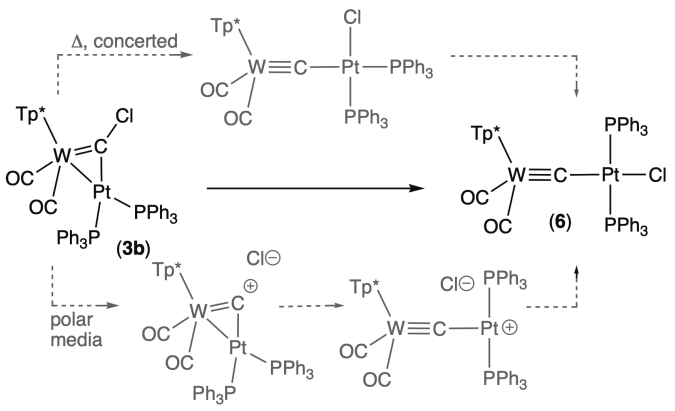

Scheme 3: Mechanistic conjecture (in grey) on the isomerism of a μ-chlorocarbyne to a μ-carbido complex.

It seems plausible that availability of protons from either moist solvents or the hydroxylic surface of the chromatographic stationary phase favours polarisation and eventual ionisation of the C–Cl bond of the μ_2-CCl ligand to generate a cationic μ_2-carbido complex, with re-association of the chloride at platinum, rather than carbon. It is of

interest that the reverse reaction, transfer of chloride to a μ_2-carbido ligand to generate a μ_2-CCl ligand, is implicit in the formation of $[Rh_2(\mu_2\text{-CCl})(\mu_2\text{-Cl})Cl(dppm)_2]$[22] from $[Rh_2(\mu_2\text{-C})Cl_2(dppm)_2]$.[62] The geometry of the μ_2-carbido ligand in the intermediate is uncertain, given that examples of bent MCM linkages have recently been isolated,[63] *i.e.*, it is not clear if assumption of a linear metallacarbyne geometry would follow or concertedly accompany chloride ionisation. The optimised synthesis of **6** involves combination of **1b** and $[Pt(\eta^2\text{-}C_2H_4)(PPh_3)_2]$ in refluxing CH_2Cl_2 for four hours.

The characterisation of **6**, which included a crystallographic analysis (Figure 14), proved straightforward given the now significant number of group 10 μ_2-carbido complexes available for comparison,[23,27a,c,64] including the structurally characterised bromo analogue $[WPt(\mu_2\text{-C})Br(PPh_3)_2(CO)_2(Tp^*)]$.[23b] The Pt–Cl bond length (2.413(1) Å) is significantly shorter than that calculated for the theoretical variant $[WPt(\mu_2\text{-C})Cl(PMe_3)_2(CO)_2(Tp)]$ (2.463 Å)[23b] despite the latter having less sterically demanding co-ligands (Tp *cf.* Tp*, PMe_3 *cf.* PPh_3). The angle observed along the carbido spine (160.12(4)°) falls well short of what would be expected for a linear *sp*-hybridised carbido, however the value calculated for the more compactly ligated $[WPt(\mu_2\text{-C})Cl(PMe_3)_2(CO)_2(Tp)]$ (174.6°) suggests that this deformation is simply a response to unfavourable inter-ligand interactions. The requisite interdigitation of adjacent phenyl and pyrazolyl groups presumably exerts deformational forces on the W–C–Pt angle and as observed for $[Rh_2(\mu_2\text{-C})Cl_2(\mu_2\text{-DMAD})(dppm)_2]$ (Rh–C–Rh = 124.7(10)°, DMAD = dimethylacetylenedicarboxylate),[63a] metal-carbido multiple bonding may be maintained even when quite dramatic bending occurs.

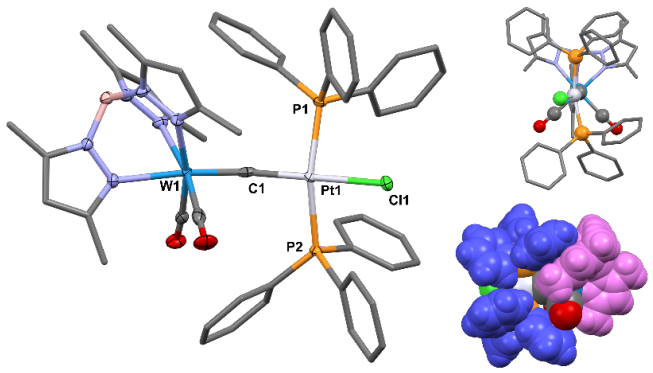

Figure 14: Molecular structure of **6** in a crystal (50% displacement ellipsoids, pyrazolyl and phenyl rings simplified with hydrogen atoms omitted for clarity). Selected bond lengths (Å), angles (°), and torsions (°): W1–C1 1.842(4), C1–Pt1 1.944(4), Pt1–Cl1 2.413(1), Pt1–P1 2.322(1), Pt1–P2 2.323(1), W1–C1–Pt1 169.0(2), P1–Pt1–P2 160.12(4), B1–W1–Pt1–P1 7.3(1). Insets: view along the W–C–Pt axis and a space-filling representation showing the clash of the encumbering phosphine (blue) and pyrazolylborate ligands (magenta).

Spectroscopic features of **6** are generally comparable to those for the previously reported bromide analogue, the standout datum being the resonance for the μ_2-carbido carbon which appears to very high frequency in the $^{13}C\{^1H\}$ NMR spectrum at δ_C = 318.8 (dd, $^2J_{PC}$ = 15 Hz). Couplings ($^1J_{PtP}$ = 3223; $^2J_{PP}$ = 443 Hz) between phosphorus (δ_P = 28.7, 23.6) and platinum (δ_{Pt} = –3718) nuclei are all consistent with the solid-state structure in which the two mutually *trans* phosphines remain chemically inequivalent due to hindered rotation about the W-C-Pt vector due to one phosphine phenyl group being locked between two pyrazolyl groups.

The facility of insertion of platinum(0) into the carbon-halogen bond of a μ_2-halocarbyne ligand should reflect the impact of co-ligands on the stability of Pt(0) *cf.* Pt(II) oxidation states. Accordingly, replacing phosphines with π-acceptor ligands might be expected to inhibit the oxidative addition process. Isonitriles are insufficiently electron withdrawing to serve this purpose, as demonstrated by the reaction of **1d** with $[Pt_3(CNC_6H_2Me_3\text{-}2,4,6)_6]$ (synthetically equivalent to '$Pt(CNC_6H_2Me_3)_2$') to afford the μ_2-carbido complex $[WPt(\mu_2\text{-C})Br(CNC_6H_2Me_3)_2(CO)_2(Tp^*)]$.[65] Nevertheless, if a freshly prepared solution of **3b** is subjected to one atmosphere of CO, a clean reaction ensues to afford the *mono*phosphine complex $[WPt(\mu_2\text{-CCl})(CO)_3(PPh_3)(Tp^*)]$ (**7**, Figure 15, Scheme 2) in which the chlorocarbyne remains intact and appears indefinitely stable and not prone to oxidative addition. The gross geometric features of **7** are comparable to those described for **3a**, **3b** and **4** above. In the case of **3b** (the precursor for **7**) the Pt–P bond length opposite the carbyne carbon is significantly (60 e.s.d.) elongated relative to that *trans* to the W–Pt bond and this *pseudo-trans* influence may well manifest a selective *trans* effect for the displacement of this particular phosphine. That said, the *ultimate* location of the introduced CO ligand *trans* to the chlorocarbyne might also arise from rotation of the '$Pt(CO)(PPh_3)$' unit so as to access the sterically least cluttered arrangement.

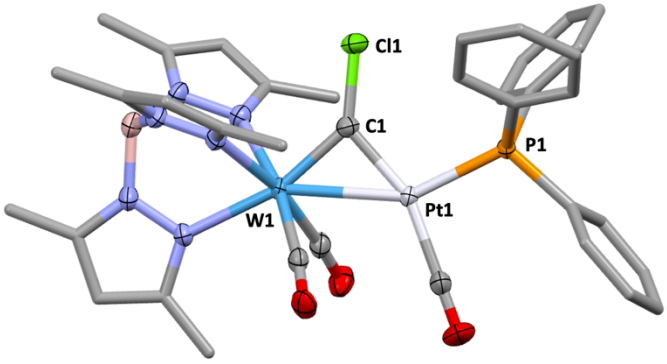

Figure 15: Molecular structure of **7** in a crystal (50% displacement ellipsoids, pyrazolyl and phenyl rings simplified with hydrogen atoms omitted for clarity).

Replacement of the phosphine by a π-acidic CO ligand is accompanied by a significant contraction of the Pt–C bond length (1.950(4) Å *cf.* 1.988, 1.965) and Pt–W (2.7732(2) Å *cf.* 2.7961(4) and 2.8078(4) Å) relative to **3b**. This, however, most likely reflects a relaxation of steric pressures from ligands on adjacent metals, given the modest variations in geometric features in the dimetallacyclopropene cores optimised for the model complexes $[MPt(\mu_2\text{-CCl})(CO)_2(L)(PMe_3)_n(Tp)]$ (M = W, L = PMe_3 **3'^{W}**; CO **7'^{W}**; M = Mo, **3'^{Mo}**, CO **7'^{Mo}**, Table 4, Fig. 11 and Fig. S20 in ESI). Whilst the bis(phosphine) derivatives $[MPt(\mu_2\text{-CCl})(CO)_2(PMe_3)_2(Tp)]$ adopt similar geometries to that observed experimentally for **3a** and **3b** such that the '$(CCl)Pt(PR_3)_2$' unit nestles between two dimethypyrazolyl groups, in the case of the tricarbonyl derivatives $[MPt(\mu_2\text{-CCl})(CO)_3(PMe_3)(Tp)]$, the '$(CCl)Pt(CO)(PR_3)$' group is rotated such that the platinum and tungsten coordination planes align (Fig. 16). Such an alignment would seem improbable for the full molecule

7 as it would bring the μ_2-CCl ligand into steric conflict with one pyrazoyl methyl substituent.

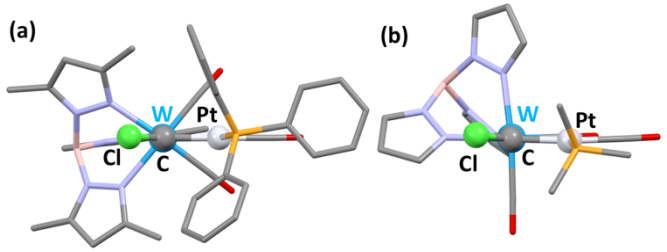

Figure 16: Relative orientations of the '(ClC)Pt(CO)(PR$_3$)' coordination planes as (a) observed experimentally for **7** and (b) derived computationally for hypothetical **7'^{W}**.

Halocarbyne Oxidation

The isolation of the high oxidation state bromocarbyne [W(≡CBr)Br$_3$(dcpe)][13c] from the reaction of [W(≡CSiPh$_3$)Br(CO)$_2$(dcpe)] with bromine prompted the question of whether oxidation of low-valent halocarbynes such as [W(≡CBr)(CO)$_2$(Tp*)] (**1d**) might be viable without rupture of the W≡C multiple bond. Treating the *bromo*carbyne complex **1b** with PhICl$_2$ does indeed lead to oxidation however two different complexes are obtained, *viz.* the known green-yellow complex [WCl$_3$(Tp*)] (**8**)[66] in which the carbyne ligand has been lost entirely, but also the blue *chloro*carbyne complex [W(≡CCl)Cl$_2$(Tp*)] (**9**) in which both the tungsten and the carbyne carbon have been chlorinated. Bromide/chloride exchange in the putative [W(≡CBr)Cl$_2$(Tp*)] intermediate presumably simply reflects the greater C–Cl *vs* C–Br bond strength.

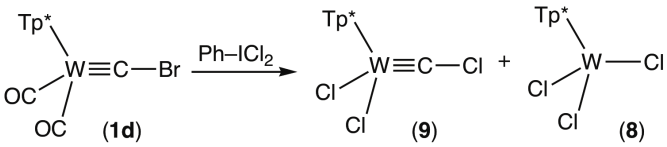

Scheme 4: Oxidative decarbonylation and halogen exchange of a bromocarbyne complex.

The complex **8** was structurally characterised revealing little of interest (Figure 17a, crystallographically imposed C_s symmetry), however the molecular structure of [W(≡CCl)Cl$_2$(Tp*)] (**9**) (Figure 17b) was more noteworthy, given the geometric data available for [M(≡CBr)(CO)$_2$(Tp*)] (M = Mo **1c**, W **1d**) but in the absence of such data for [W(≡CCl)(CO)$_2$(Tp*)] (**1b**). Exhaustive attempts to secure crystallographic grade crystals of either **1b** or its molybdenum congener **1a** from a multitude of solvent combinations provided only weakly diffracting specimens (including synchroton measurement), one of which was isomorphous with **1d**. Only half the C_s-symmetric molecule **9** is unique due to a crystallographic mirror plane (x, $^1/_4$, z) that includes the chlorocarbyne and one pyrazolyl ring.

The geometrical impacts of tungsten oxidation may be assessed by consideration of experimental data for (i) [W(≡CCl)(CO)$_2$(Tp*)] (**1b**) *vs* [W(≡CCl)Cl$_2$(Tp*)] (**9**). This pair of carbyne complexes joins a small number of octahedral Tp or Tp* carbyne complexes for which data are available for both the low-valent dicarbonyl and high-valent dihalo examples.[67-70] Carbon-13 NMR spectroscopic and crystallographic data of interest for these complexes are collected in Table 6 whilst computationally-derived data for the model complexes [W(≡CCl)(CO)$_2$(Tp)] (**1b'**) and [W(≡CCl)Cl$_2$(Tp)] (**9'**) are included in Table 2.

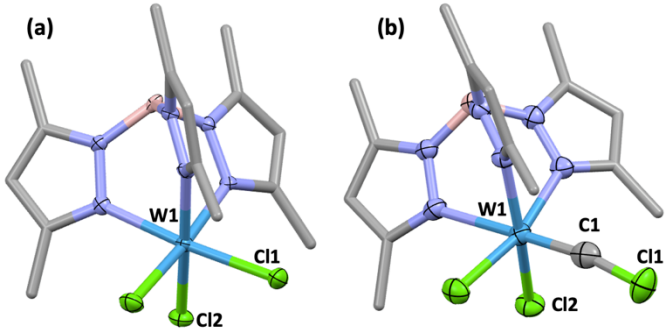

Figure 17. Molecular structures of (a) [WCl$_3$(Tp*)] (**8**) and (b) [W(≡CCl)Cl$_2$(Tp*)] (**9**) in crystals (50% displacement ellipsoids, pyrazolyl rings simplified with hydrogen atoms omitted for clarity).

Whilst the computational economy afforded by pruning the Tp* ligand to Tp has been found to have a negligible effect on the electronic features and the resulting M≡C bond lengths for related complexes,[32] it is expected to impact to some degree on inter-ligand angles. Firstly, Table 6 reveals that quite generally, oxidation of the tungsten centre results in a substantial shift in the carbyne resonance to low-frequency (35–50 ppm), with the effect being least pronounced for amino derivatives bearing positively mesomeric (***M***$^+$) trigonal nitrogen substituents. For each comparative pair, the W≡C bond contracts upon oxidation with the exception again of the amino derivatives. The replacement of two CO ligands with short W–C bond lengths *cf.* longer W–Cl bonds may well allow closer approach of the carbyne carbon to tungsten, whilst the recalcitrance of aminocarbynes may be attributed to contributions of a zwitterionic 2-azavinylidene canonical description with reduced W-C bond order being more relevant to the more oxidised tungsten. With reference to the data in Table 2, other than reproducing experimental observations for geometric changes (**2b** *cf.* **9**, Table 6) it is noteworthy that halogenation of **2b'** to **9'** results in an increase in WC bond order (from 2.450 to 2.671) but no change in that of the C–Cl bond (1.315 to 1.318) and this is reflected in an increase in the frequency (1248 cm^{-1}) calculated for the vibrational mode that is primarily associated with $\nu_{W\equiv C}$ stretching. Perhaps most notable, however is that whilst oxidation of the tungsten centre results in a substantial increase in positive charge (+0.945 to +1.474), the charge on the chloride is unchanged and near to neutral (+0.065), while the charge on the carbyne carbon (–0.410) is essentially unchanged from that of **2b'** (–0.395).

That remarkably little variation is noted between the W≡CCl linkages of **2b'** and **9'** calls for closer inspection with respect to the Fischer-Schrock carbyne dichotomy about which much has been written.[71,72] In short, so-called Fischer-type carbynes typically involve low-valent metal centres that are coordinatively saturated with π-acidic co-ligands such that the carbyne is prone to nucleophilic attack (*cf.* the 18-electron metal centre). Schrock-type carbynes involve high-valent metal centres, the coordinative unsaturation of which is often, but not always, stabilised by π-donor co-ligands, with the carbyne carbon displaying nucleophilic character and the metal centre being prone to addition of ligands/nucleophiles. Accordingly, the carbyne couples of the form [W(CR)L$_2$(Tp)] from Table 6 which

differ only in the level of coordinative (un)saturation and the nature of L (π-acidic CO *cf.* π-basic halide) provide a tidy platform *ceteris paribus* for exploring this dichotomy.

Table 6. Selected spectroscopic and crystallographic data for redox couplet complexes of the form [W(≡CR)L_2(Tp')] (R = Cl, Mes, Xyl, Ph, C_3[a]; L = CO, Cl, Br; Tp' = Tp, Tp*)

R	L	Tp'	δ_C [ppm]	r_{WC} [Å]	WCR [°]	*TR*[b]
Cl	CO	Tp*	205.6	-	-	-
Cl	Cl	Tp*	240.9	1.829(8)	171.1(4)	1.098
Mes	CO[67]	Tp	288.5	1.825(5)	173.9(4)	1.038
Xyl	Cl[67]	Tp	326.5	1.800(11)	176.7(11)	1.096
Tol	CO[69a]	Tp*	279.6	1.829(*c*)	163.2(*c*)	1.036
Ph	Cl[69b]	Tp*	327.4	1.783(9)	168.0(8)	1.093
C_3	CO[68a]	Tp*	242.8	1.826(3)	175.6(3)	1.025
C_3	Cl[68b]	Tp*	283.6	1.811(8)	175.7(9)	1.103
NEt_2	CO[70b]	Tp*	248.6	*c*	*c*	–
NPh_2	CO[70a]	Tp*	235.5	1.837(3)	176.5(3)	1.037
NEt_2	Br[74c]	Tp*	266.5	1.963(8)	174.5(5)	1.098

[a]Mes = $C_6H_2Me_3$-2,4,6, Xyl = $C_6H_3Me_2$-2,6, Tol = C_6H_4Me-4, C_3 = ½ μ-C_6 in [W_2(μ-C_6)$(CO)_4$(Tp*)$_2$].[68a] [b]***TR*** = 2*r*(WN_{trans})/Σ*r*(WN_{cis}). [c]Not reported.

Figure 18 presents the frontier molecular orbitals of interest for **2b'** and **9'**. As discussed above for the molybdenum complexes [Mo(≡CX)$(CO)_2$(Tp)] (X = F, Cl, Br, I), for the low-valent example **2b'**, the HOMO essentially comprises the tungsten d_{xy} orbital (W–CCl vector as '*z*') involved in retrodatively binding the two CO ligands. Thus the π-components of the W≡C multiple bond comprise the near-degenerate HOMO-1 and 2 pair of orbitals and perhaps surprisingly, these are very similar both in energy and topology to the HOMO and HOMO-1 calculated for the high-valent example **9'**. The LUMO and LUMO+1 of **2b'** are W–C π-antibonding in nature with quite substantial contributions from the carbyne carbon p_x and p_y orbitals. This is consistent with nucleophilic attack at the carbyne carbon of Fischer-type carbynes in frontier-orbital-controlled reactions.[73] In contrast, the LUMO of **9'** is predominantly metal-based, being primarily the same d_{xy} orbital that constituted the HOMO of **2b'**. This orbital is orthogonal to the W≡C bond and accordingly, in the present system, the tendency of nucleophiles to attack the metal centre of **9'** and of electrophiles to attack the metal in **2b'** simply relates to the occupancy (d^4 or d^6 in the CR^+ formalism) of this orbital, with the frontier orbitals of the WC bond itself being remarkably similar for both the 'Fischer' and 'Schrock' variants. The minimal contribution of charge control to regioselectivity follows from the data in Table 2 which reveal almost identical charges on the carbyne carbons of both **2b'** and **9'** but a significant increase in positive charge on tungsten for **2b'** (1.474 *cf.* 0.945 for **2b'**).

The regioselectivity of nucleophilic *cf.* electrophilic attack may also be interpreted with reference to Fukui (frontier) functions, f^+ and f^-, respectively,[74,75] and these parameters have recently been considered for a range of late transition metal alkylidyne complexes to explore the regioselectivity of [2+3] (*pseudo*-Huisgen) cycloaddition of azides.[76] Table 7 presents both f^- and f^+ functions for both **2b'** and **9'**. Considering first electrophilic attack, the tungsten centre of **2b'** is by a substantial margin the most attractive site for electrophilic attack (f^- = 0.368) with the carbonyl oxygen atoms presenting the next but far less attractive sites, consistent with the HOMO being metal-based and not associated with the halocarbyne. In contrast, with the metal d_{xy} orbital being unoccupied for **9'**, the nucleophilicity of the metal is significantly reduced (f^- = 0.143), though still greater than for the carbyne carbon, while the terminal chloride has the greatest value for f^-. For nucleophilic attack, the carbyne carbon of **2b'** has the highest f^+ value, however the metal centre and even the carbon of the carbonyl co-ligands present alternative sites for nucleophiles. The high-valent **9'** however shows a clear preference (f^+ = 0.218) for nucleophilic attack at the metal as suggested by the substantial contribution of the d_{xy} orbital to the LUMO (Figure 18).

Table 7. Atom-Condensed Fukui Functions for Electrophilic (f^-) and Nucleophilic (f^+) attack at [W(≡CCl)L_2(Tp)] (L = CO **2b'**, Cl **9'**)

Electrophilic Attack	f^-(W)	f^-(C)	f^-(Cl)	f^-(**C**O)	f(C**O**)
[W(≡CCl)$(CO)_2$(Tp)] (**2b'**)	0.368	0.047	0.105	0.019	0.118
[W(≡CCl)Cl_2(Tp)] (**9'**)	0.143	0.091	0.173	–	–
Nucleophilic Attack	f^+(W)	f^+(C)	f^+(Cl)	f^+(**C**O)	f^+(C**O**)
[W(≡CCl)$(CO)_2$(Tp)] (**2b'**)	0.139	0.160	0.022	0.107	0.095
[W(≡CCl)Cl_2(Tp)] (**9'**)	0.218	0.113	0.100	–	–

Conclusions

A range of μ_2-bromo- and chlorocarbyne heterobimetallic complexes have been prepared in which the carbyne bridges between tungsten and either gold(I) or platinum(0), including a trimetallic bis(μ-carbyne) example. This significantly increases the range of μ_2-halocarbynes, of which only four previous *homobimetallic* examples [W_2(μ_2-CCl)(μ_2-Cl)$_2Cl_5$]$_n$[21a] , [Ru_2(μ_2-CCl)(μ_2-Cl)Cl_2(η^5-C_5Me_5)$_2$][21b] and [Rh_2(μ_2-CX)(μ_2-X)X_4(dppm)$_2$] (X = Cl, Br)[22] had been structurally characterised. These are seen as intercepted intermediates in the insertion of metals into the C-halogen bond (oxidative addition), although an unexpected solvent polarity dependence suggests that the process might not be concerted. In any event, this may be retarded by inclusion of π-acid co-ligands on platinum that presumably destabilise the higher oxidation state resulting from oxidative addition. The LUMO of various heterobimetallic μ_2-halocarbynes includes considerable contribution from the carbyne carbon such that these complexes might be expected to promise utility as intermediates for the synthesis of other types of μ_2-carbyne complexes via nucleophilic substitution.

Oxidation of a low-valent terminal bromocarbyne [W(≡CBr)$(CO)_2$(Tp*)] to a high-valent chlorocarbyne derivative [W(≡CCl)Cl_2(Tp*)] allowed interrogation *ceteris paribus* of the Fischer-Schrock carbyne dichotomy as it applies to halocarbynes. This analysis concluded that disparities in reactivity have more to do with the energy and occupancy of a metal centred orbital ('d_{xy}') that is actually orthogonal to the MC multiple bond, the frontier orbitals of which are rather similar in energy and topology.

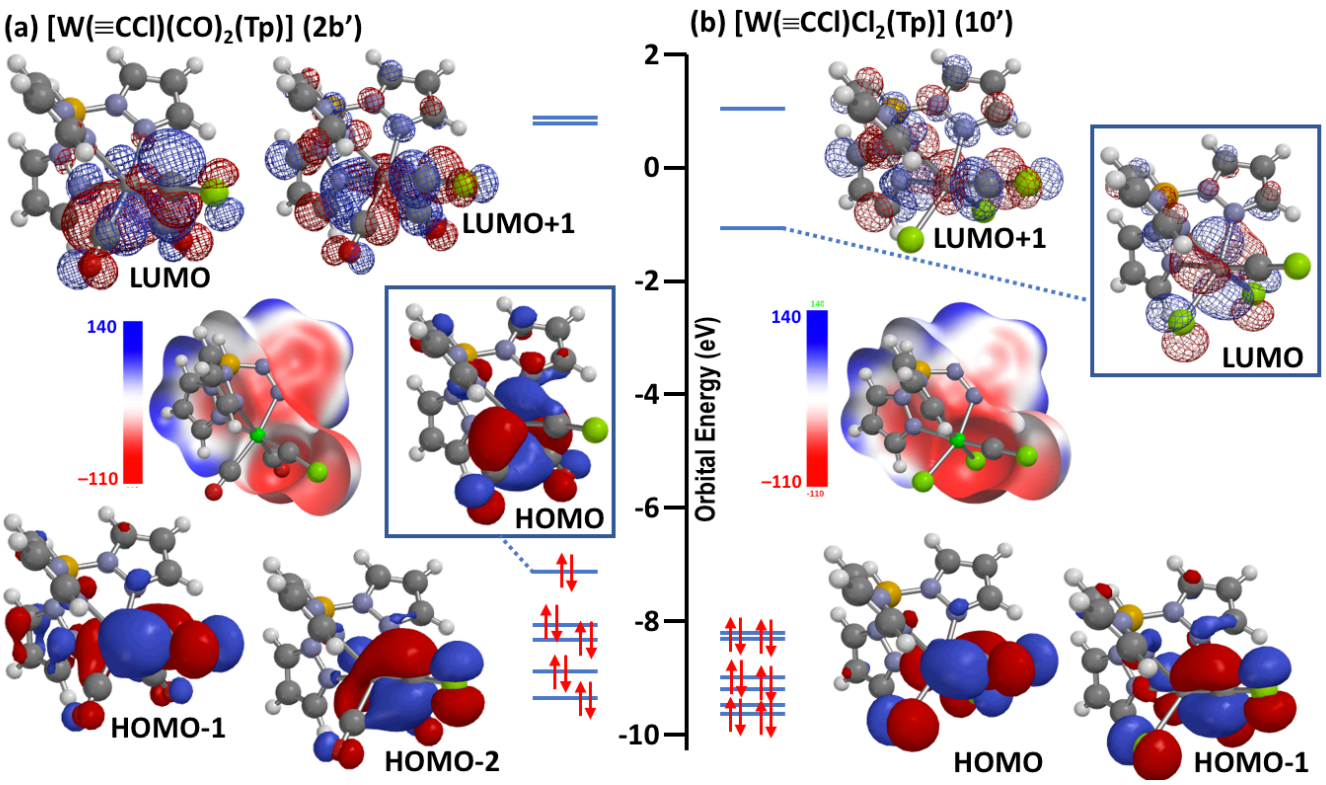

Figure 18. Frontier orbitals of interest (isovalue = 0.032; DFT:ωB97X-D/6-31G*/LANL2Dζ) for the complexes (a) [W(≡CCl)(CO)$_2$(Tp)] (**2a'**) and (b) [W(≡CCl)Cl$_2$(Tp)] (**9'**) with insets showing electrostatic potential surfaces (-110 to 140 kJ).

Acknowledgements

We gratefully acknowledge the Australian Research Council (DP190100723 and DP200101222) for funding.

Conflicts of Interest

There are no conflicts to declare.

Experimental

General experimental details and instrumentation, synthetic methods, spectroscopic data, selected spectra, cartesian coordinates and computational details are provided in the accompanying Electronic Supporting Information.

Conflicts of interest

The authors have no conflicts of interest to declare.

Author Contributions

LKB was responsible for the design and execution of the experimental research, the acquisition and critical analysis of the characterisational data and compilation of the original draft. RDD, RYK, EEN and CSO contributed to the original synthesis and characterisation of selected compounds. AFH was responsible for funding acquisition, project conceptualisation and administration, validation and refinements to the manuscript.

Notes and references

1 Reviews: (a) E. O. Fischer, *Adv. Organomet. Chem.*, 1976, **14**, 1-32. (b) R. R. Schrock, *J. Chem. Soc., Dalton Trans.*, 2001, 2541-2550. (c) R. R. Schrock, *Chem. Rev.*, 2002, **102**, 145-179. (d) R. R. Schrock and C. Czekelius, *Adv. Synth. Cat.*, 2007, **349**, 55-77 (e) R. A. Manzano and A. F. Hill, *Adv. Organomet. Chem.*, 2019, **72**, 103-171. (f) H. Ehrhorn and M. Tamm, *Chem. Eur. J.*, 2019, **25**, 3190-3208. (g) A. Fürstner and P. W. Davies, *Chem. Commun.*, 2005, 2307-2320. (h) L. M. Caldwell, *Adv. Organomet. Chem.* 2008, **56**, 1-94.

2 (a) E. O. Fischer, G. Huttner, W. Kleine and A. Frank, 1975, **14**, 760-760; (b) J. L. Pombeiro, M. F. C. Guedes da Silva and R. A. Michelin, *Coord. Chem. Rev.*, 2001, **218**, 43-74.

3 (a) E. O. Fischer, H. Hollfelder, P. Friedrich, F. R. Kreissl and G. Huttner, *Angew. Chem., Int. Ed. Engl.,* 1977, **16**, 401-402; (b) G. M. Jamison, P. S. White, D. L. Harris and J. L. Templeton in *Transition Metal Carbyne Complexes*, Ed. F. R. Kreissl, *NATO ASI Series C*, 1993, **392**, 201-218. (c) A. F. Hill, J. S. Ward and Y. Xiong, *Organometallics*, 2015, **34**, 5057–5064.

4 (a) H. P. Kim and R. J. Angelici, *Adv. Organomet. Chem.*, 1987, **27**, 51-111. (b) A. Mayr and H. Hoffmeister, *Adv. Organomet. Chem.*, 1991, **32**, 227-324.

5 W. W. Greaves, R. J. Angelici, B. J. Helland, R. Klima and R. A. Jacobson, *J. Am. Chem. Soc.*, 1979, **101**, 7618-7620.

6 (a) T. Desmond, F. J. Lalor, G. Ferguson and M. Parvez, *J. Chem. Soc., Chem. Commun.*, 1984, 75-77. (b) B. J. Frogley, A. F. Hill and L. J. Watson, *Chem. Eur. J.*, 2020, **26**, 12706-12716. (c) R. L. Cordiner, A. F. Hill and J. Wagler, *Organometallics*, 2008, **27**, 4532-4540. (d) I. A. Cade, A. F. Hill, C. M. A. McQueen,

Organometallics, 2009, **28**, 6639-6641. (e) L. M. Caldwell, R. L. Cordiner, A. F. Hill and J. Wagler, *Organometallics*, 2010, **29**, 1526-1529. (f) A. F. Hill and C. M. A. McQueen, *Organometallics,* 2012, **31**, 2482-2485. (g) L. M. Caldwell, A. F. Hill, R. Stranger, R. N. L. Terrett, K. M. von Nessi, J. Ward and A. C. Willis, *Organometallics*, 2015, **34**, 328-334. (h) B. J. Frogley, A. F. Hill, R. A. Manzano and M. Sharma, *Chem. Commun.*, 2018, **54**, 1702-1705. (i) I. A. Cade, A. F. Hill and C. M. A. McQueen, *Dalton Trans.*, 2019, **48**, 2000-2012. (j) B. J. Frogley, T. L. Genet, A. F Hill and C. S. Onn, *Dalton Trans.*, 2019, 48, 7632-7643. (k) B. J. Frogley, A. F. Hill and C. S. Onn, Dalton Trans., 2019, **48**, 11715-11723. (l) A. F. Hill and L. J. Watson, *Chem. Commun.*, 2020, **56**, 2356-2359. (m) B. J. Frogley, A. F. Hill, C. S. Onn and L. J. Watson, *Angew. Chem., Int. Ed.*, 2019, **58**, 15349-15353. (n) B. J. Frogley, A. F. Hill and L. J. Watson, *Dalton Trans.*, 2019, **48**, 12598-12606.

7 (a) A. L. Colebatch, B. J. Frogley, A. F. Hill and C. S. Onn, *Chem. Eur. J.*, 2021, **27**, 5322-5343.

8 (a) L. Weber, I. Schumann, T. Schmidt, H.-G. Stammler and B. Neumann, *Z. Anorg. Allg. Chem.,* 1993, **619**, 1759-1764. (b) L. Weber, I. Schumann, H.-G. Stammler and B. Neumann, *Chem. Ber.*, 1994, **127**, 1349-1353. (c) L. Weber, I. Schumann, M. H. Scheffer, H.-G. Stammler and B. Neumann, *Z. Naturforsch. B,* 1997, **52**, 655-662. (d) L. Weber, G. Dembeck, R. Boese and D. Bläser, *Chem. Ber.*, 1997, **130**, 1305-1308. (e) L. Weber, G. Dembeck, H.-G. Stammler and B. Neumann, *Eur. J. Inorg. Chem.,* 1998, 579-582. (f) L. Weber, G. Dembeck, H.-G. Stammler and B. Neumann, M. Schmidtmann and A. Müller, *Organometallics*, 1998, *17*, 5254-5259. (g) L. Weber, G. Dembeck, P. Lönneke, H.-G. Stammler, B. Neumann, *Organometallics* 2001, **20**, 2288-2293. (h) L. Weber, G. Dembeck, R. Boese, D. Bläser, *Organometallics* 1999, **18**, 4603-4607.

9 (a) R. L. Cordiner, P. A. Gugger, A. F. Hill and A. C. Willis, *Organometallics*, 2009, **28**, 6632-6635. (b) A. L. Colebatch and A. F. Hill, *J. Am. Chem. Soc.*, 2014, **136**, 17442-17445.

10 (a) R. L. Cordiner, A. F. Hill and J. Wagler, *Organometallics*, 2008, **27**, 5177-5179.

11 (a) E. S. Borren, A. F. Hill, R. Shang, M. Sharma and A. C. Willis, *J. Am. Chem. Soc.*, 2013, **135**, 4942–4945; (b) A. Reinholdt, J. Bendix,A. F. Hill and R. A. Manzano, *Dalton Trans.*, 2018, **47**, 14893-14896.

12 (a) B. J. Frogley and A. F. Hill, *Chem. Commun.,* 2018, **54**, 7649-7652. (b) B. J. Frogley and A. F. Hill, *Chem. Commun.*, 2018, **54**, 2126-2129. (c) A. L. Colebatch and A. F. Hill, *Dalton Trans.*, 2017, **46**, 4355-4365. (d) A. L. Colebatch, Y.-S. Han, A. F. Hill, M. Sharma, R. Shang and J. S. Ward, *Chem. Commun.*, 2017, **53**, 1832-1835. (e) A. L. Colebatch and A. F. Hill, *Organometallics*, 2016, **35**, 2249-2255. (f) A. L. Colebatch, A. F. Hill and M. Sharma, *Organometallics*, 2015, **34**, 2165-2182. (g) B. J. Frogley and A. F. Hill, *Dalton Trans.*, 2022, **51**, 1907-1917. (h) B. J. Frogley, A. F. Hill and R. M. Kirk, *Chem. Commun.,* 2021, **57**, 8770-8773. (i) B. J. Frogley, A. F. Hill, R. Shang, M. Sharma and A. C. Willis, *Chem. Eur. J.*, 2020, **26**, 8819-8827. (j) B. J. Frogley and A. F. Hill, *Chem. Commun.,* 2018, **54**, 12373-12376.

13 (a) F. J. Lalor, T. J. Desmond, G. M. Cotter, C. A. Shanahan, G. Ferguson, M. Parvez and B. Ruhl, *J. Chem. Soc., Dalton Trans.*, 1995, 1709-1726. (b) T. Desmond, F. J. Lalor, G. Ferguson and M. Parvez, *J. Chem. Soc., Chem. Commun.*, 1983, 457-459 (c) A. F. Hill and R. Y. Kong, *Chem. Commun*, 2017, **53**, 759-762.

14 (a) W. T. Dent, L. A. Duncanson, R. G. Guy, H. W. B. Reed and B. L. Shaw, *Proc. Chem. Soc.*, 1961, 169-169. (b) K. Bartl, R. Boese and G. Schmid, *J. Organomet. Chem.,* 1981, **206**, 331-345.

15 D. Seyferth, C. N. Rudie, J. S. Merola and D. H. Berry, *J. Organomet. Chem.*, 1980, **187**, 91-102 and preceding papers in the series *"Organocobalt cluster complexes"* referred to therein, including D. Seyferth, *Adv. Organomet. Chem.*, 1976, **14**, 97-144.

16 (a) J. B. Keister and T. L. Horling, *Inorg. Chem.*, 1980, **19**, 2304-2307. (b) M. I. Bruce, P. A. Humphrey, B. W. Skelton and A. H. White, *Z. Anorg. Allg. Chem.*, 2011, **637**, 676-681. (c) D.-Y. Jan, D. P. Workman, L.-Y.Hsu, J. A. Krause and S. G. Shore, Inorg. Chem., 1992, **31**, 5123-5131.

17 D. N. Duffy, M. M. Kassis and A. D. Rae, *J. Organomet. Chem.,* 1993, **460**, 97-104.

18 (a) H. Huang, R. P. Hughes and A. L. Rheingold, *Dalton Trans.* 2011, **40**, 47-55. (b) H. Huang, R. P. Hughes, C. R. Landis and A. L. Rheingold, *J. Am. Chem. Soc.*, 2006, **128**, 7454-7455.

19 C. J. Pell, Y. Zhu, R. Huacuja, D. E. Herbert, R. P. Hughes and O. V. Ozerov, *Chem. Sci.*, 2017, **8**, 3178-3186.

20 F. G. A. Stone, *Angew. Chem., Int. Ed. Engl.*, 1984, **23**, 89-99.

21 (a) J. Beck and F. Wolf, *Z. Anorg. Allg. Chem.*, 2002, **628**, 1453-1454. (b) T. Takao and K. Seki, *Organometallics*, 2021, **40**, 467-471. (c) G. I. Novikov, N. V. Andreeva and O. G. Polyachenok, *Russ. J. Inorg. Chem.*, 1961, **6**, 1019.

22 H. J. Barnett and A. F. Hill, *Chem Commun.* 2019, **55**, 1734-1737.

23 (a) W. Knauer and W. Beck, *Z. Anorg. Allg. Chem.*, 2008, **634**, 2241-2245. (b) L. K. Burt and A. F. Hill, *Dalton Trans*, 2020, **49**, 8143-8161.

24 (a) T. V. Ashworth, J. A. K. Howard, F. G. A. Stone, *Chem. Commun.*, 1979, 42-46. (b) J. C. Jeffery, D. B. Lewis, G. E. Lewis, M. J. Parrott and F. G. A. Stone, *J. Chem. Soc., Dalton Trans.* 1986, 1717-1722. (c) M. J. Attfield, J. A. K. Howard, A. N. de M. Jelfs, C. M. Nunn and F. G. A. Stone, *Chem. Commun.*, 1986, , 918-920. (d) S. H. F. Becke, M. D. Bermudez, N. H. Tran-Huy, J. A. K. Howard, O. Johnson and F. G. A. Stone, *J. Chem. Soc., Dalton Trans.,* 1987, 1229-1234. (e) N. Carr, M. C. Gimeno and F. G. A. Stone, *J. Chem. Soc., Dalton Trans*., 1990, 2617-2624. (f) T. V. Ashworth, J. A. K. Howard and F. G. A. Stone, *J. Chem. Soc., Dalton Trans.,* 1980, 1609-1614. (g) P. K. Byers, N. Carr and F. G. A. Stone, *J. Chem. Soc., Dalton Trans.,* 1990, 3701-3708.

25 (a) B. J. Frogley and A. F. Hill, *Angew. Chem., Int. Ed.*, 2019, **58**, 8044-8048. (b) A. R. Delaney, B. J. Frogley and A.F.Hill, *Dalton Trans.*, 2019, **48**, 13674-13684.

26 H. Bera, H. Braunschweig, R. Dörfler and K. Radacki, *Dalton Trans.*, 2008, 440-443.

27 (a) C. S. Onn, A. F. Hill and A. Olding, *Dalton Trans.*, 2020, **49**, 12731-12741. (b) A. F. Hill and M. Sharma, *Organometallics*, 2012, **31**, 2538-2542 (c) L. K. Burt, R. L. Cordiner, A. F. Hill, R. A. Manzano and J. Wagler, *Chem. Commun.*, 2020, **56**, 5673-5676.

28 (a) A. E. Enriquez, P. S. White and J. L. Templeton, *J. Am. Chem. Soc.,* 2001, **123**, 4992-5002; (b) T. J. Desmond, F. J. Lalor, G. Ferguson, M. Parvez and T. Wieckowski, *Acta Crystallogr.* 1990, **C46**, 59-61.

29 Because Fischer's first carbyne synthesis involved electrophilic MeO^- abstraction from a neutral :C(OMe)Ph ligand, the perspective that the resulting carbyne ligand is cationic has endured and many carbyne complexes have analogous nitrosyl complexes. The alternative perspective considers two α-hydrogen abstractions to occur from a monoanionic CH_2R alkyl ligand to provide a trianionic carbyne. The actual charge calculated for a carbyne carbon, which is always negative, is typically between 0 and –1 (*e.g.*, see Table 2). Green's covalent bond classification method considers a carbyne to be an X_3 ligand: (a) M. L. H. Green, *J. Organomet. Chem.*, 1995, **500**, 127–148. (b) M. L. H. Green and G. Parkin, *J. Chem. Ed.*, 2014, **91**, 807-816.

30 (a) J. Y. Saillard, D. Grandjean, P. Caillet and A. Le Beuze, *J. Organomet. Chem.*, 1980, **190**, 371-379. (b) J. C. Green, A. L. Hector, A. F. Hill and J. D. E. T. Wilton-Ely, *Organometallics*, 2008, **27**, 5548–5558. (c) Z. Zhang, Q.-S. Li, Y. Xie and R. B.

King, *Inorg. Chim. Acta* **2011**, *375*, 193-204. (d) A. Peng, X. Zhang, Q.-S. Li, R. B. King and H. F. Schaefer III, *New J. Chem.* 2013, **37**, 775-783. (e) Z. Zhang, L. Pu, Q.-S. Li and R. B. King, *New J. Chem.* 2014, **38**, 4282-4289. (f) H. Gong, Q. Luo, Q.-S. Li, Y. Xie, R. B. King and H. F. Schaefer III, *Inorg. Chem.* 2015, **54**, 132-142.

31 (*a*) R. B. King, A. Efraty and W. M. Douglas, *J. Organomet. Chem.*, 1973, **60**, 125-137. (*b*) J. T. Malito, R. Shakir and J L. Atwood, *J. Chem. Soc., Dalton Trans.*, 1980, 1253-1258.

32 B. J. Frogley, A. F. Hill and R. M. Kirk, *Chem. Commun.*, 2021, **57**, 8770-8773.

33 (a) B. J. Frogley and A. F. Hill, *Chem. Commun.*, 2021, **57**, 13353-13356. (b) A. F. Hill and R. A. Manzano, *Dalton Trans.*, 2019, **48**, 6596-6610.

34 (a) C. S. Kraihanzel and F. A. Cotton, I*norg. Chem.* 1963, **2**, 533–540; (b) F. A. Cotton and C. S. Kraihanzel, *J. Am. Chem. Soc.*, 1962, **84**, 4432-4438.

35 (a) J. P. Merrick, D. Moran and L. Radom, *J. Phys. Chem. A* 2007, **111***,* 11683-11700. (b) C. Y. Lin, M. W. George and P. M. W. Gill, *Aust. J. Chem.*, 2004, **57**, 365-370.

36 M. D. Halls, J. Velkovski and H. B. Schlegel *Theor. Chem. Acc.,* 2001, **105**, 413-421.

37 R. L. Jacobsen, R. D. Johnson, K. K. Irikura and R. N. Kacker, *J. Chem. Theory Comput.* 2013, **9**, 951−954.

38 Computational Chemistry Comparison and Benchmark Data Base (Release 21, August 2020) of the National Institute of Standards and Technology.

39 H. Burger, W. Schneider, S. Sommer, W. Thiel and H. Willner, *J. Chem Phys*., 1991, **95**, 5660-5669.

40 G. Cavallo, P. Matrangolo, R. Milani, T. Pilati, A. Priimagi, G. Resnati and G. Terraneo, *Chem. Rev.*, 2016, **116**, 2478–2601.

41 Though not strictly iodocarbynes as such, Reinholdt and Bendix have described diiodo and tetraiodocarbyne ligands $[Ru\{C(I_2)\}Cl_2(PCy_3)_2]$ and $[Ru\{C(I_2)_2\}Cl(NCO)(PCy_3)_2]$: A. Reinholdt, T. Vosch and J. Bendix, *Angew. Chem., Int. Ed.,* 2016, **55**, 12484-12487.

42 R. L. Cordiner, A. F. Hill and J. Wagler, *Organometallics*, 2008, **27**, 4532–4540.

43 R. Hoffmann, *Angew. Chem., Int. Ed. Engl*., 1982, **21**, 711-724

44 (a) F. G. A. Stone, *Angew. Chem., Int. Ed. Engl*., 1984, **23**, 89-99. (b) S. A. Brew and F. G. A. Stone, *Adv. Organomet. Chem.*, 1993, **35**, 135-86. (c) J. E. Goldberg, D. F. Mullica, E. L. Sappenfield and F. G. A. Stone, *J. Chem. Soc., Dalton Trans.,* 1992, 2495-502 and previous parts of the series *"Chemistry of Polynuclear Metal Complexes with Bridging Carbene or Carbyne Ligands."*.

45 (a) S. J. Dossett, A. F. Hill, J. A. K. Howard, B. A. Nasir, T. P. Spaniol, P. Sherwood and F. G. A. Stone, *J. Chem. Soc., Dalton Trans.*, 1989, 1871-1878. (b) S. J. Dossett, A. F. Hill, J. C. Jeffery, F. Marken, P. Sherwood and F. G. A. Stone, *J. Chem. Soc., Dalton Trans.*, 1988, 2453-2465.

46 (a) S. Chaona, F. J. Lalor, G. Ferguson and M. M. Hunt, *J. Chem. Soc., Chem. Commun.*, 1988, 1606-1608. (b) F. J. Lalor and S. A. O'Neill, J. *Organomet. Chem.,* 2003, **684**, 249-265.

47 (a) M. Etienne, P. S. White and J. L. Templeton, *J. Am. Chem. Soc.*, 1991, **113**, 2324-2325. (b) G. M. Jamison, P. S. White and J. L. Templeton, *Organometallics*, 1991, **10**, 1954-1959. (c) B. E. Woodworth and J. L. Templeton, J. L. *J. Am. Chem. Soc.,* 1996, **118**, 7418-7419. (d) B. E. Woodworth, D. S. Frohnapfel, P. S. White and J. L. Templeton, *Organometallics*, 1998, **17**, 1655-1662. (e) K. C. Stone, P. S. White and J. L. Templeton, *J. Organomet. Chem.*, 2003, **684**, 13-19. (f) K. C. Stone, G. M. Jamison, P. S. White and J. L. Templeton, *Organometallics*, 2003, **22**, 3083-3095. (g) K. C. Stone, G. M. Jamison, P. S. White and J. L. Templeton, *Inorg. Chim. Acta,* 2002, **330**, 161-172. (h) A. E. Enriquez and J. L. Templeton, *Organometallics*, 2002, **21**, 852-863

48 (c) B. J. Frogley, A. F. Hill and S. S. Welsh, *Dalton Trans.*, 2021, **50** 15502-15523. (d) B. J. Frogley, A. F. Hill and S. S. Welsh, *Chem. Commun.*, 2021, **57**, 13353-13356. (e) B. J. Frogley, A. F. Hill and A. Seitz, *Chem. Commun.*, 2020, **56**, 3265-3268.

49 A. F. Hill, J. M. Waters, W. R. Roper and A. H. Wright, *J. Am. Chem. Soc.,* 1983, **105**, 5939-5940.

50 (a) G. R. Clark, C. M. Cochrane, W. R. Roper and L. J. Wright, *J. Organomet. Chem.*, 1980, **199**, C35-C38. (b) G. A. Carriedo, J. C. Jeffery and F. G. A. Stone, *J. Chem. Soc., Dalton Trans.*, 1984, 1597-1603. (c) G. A. Carriedo, V. Riera, G. Sánchez and X. Solans, *J. Chem. Soc., Dalton Trans.*, 1988, 1957-1962. (d) C. E. Strasser, S. Cronje and H. G. Raubenheimer, *New J. Chem.*, 2010, **34**, 458-469. (e) A. L. Colebatch and A. F. Hill, *Dalton Trans*, 2017, **46**, 4355-4365. (f) B. J. Frogley, A. F. Hill and C. S. Onn, *Dalton Trans.*, 2019, **48**, 11715-11723.(g) B. J. Frogley, A. F. Hill and L. J. Watson, *Chem. Commun.*, 2019, **55**, 14450-14453. (h) B. J. Frogley and A. F. Hill, *Dalton Trans.*, 2020, **49**, 12390-12400 (i) X. Zhou, Y. Li, Y. Shao, Y. Hua, H. Zhang, Y.-M. Lin and H. Xia, *Organometallics,* 2018, **37**, 1788-1794.

51 B. Cordero, V. Gómez, A. E. Platero-Prats, M. Revés, J. Echeverría, E. Cremades, F. Barragán and S. Alvarez, *Dalton Trans.*, 2008, 2832-2838

52 P. Pyykkö; S. Riedel and M. Patzschke, *Chem. Eur. J.*, 2005, **11**, 3511–3520.

53 P. Pyykkö and M. Atsumi, *Chem. Eur. J.*, 2009, **15**, 12770–12779.

54 (a) M. Green, J. A. K. Howard, A. P. James, C. M. Nunn, F. G. A. Stone, *J. Chem. Soc., Chem. Comm.*, 1984, 1113-1115. (b) M. Green, J. A. K. Howard, A. P. James, C. M. Nunn and F. G. A. Stone, *J. Chem. Soc., Dalton Trans.*, 1987, 61-72.

55 (a) P. Macchi, L. Garlaschelli and A. Sironi, *J. Am. Chem. Soc*. 2002, **124**, 14173–14184. (b) R. H. Crabtree and M. Lavin, *Inorg. Chem*. 1986, **25**, 805–812. (c) S. R. Parmalee and N. P. Mankad, *Dalton Trans.*, 2015, **44**, 17007-17014.

56 (a) A. Amgoune and D. Bourissou, *Chem. Commun.*, 2011, **47**, 859-871. (b) H. Braunschweig and R. D. Dewhurst, *Dalton Trans.* 2011, **40**, 549-558.

57 B. M. Still, P. G. A. Kumar, J. R. Aldrich-Wright and W. S. Price, *Chem. Soc. Rev.*, 2007, **36**, 665–686.

58 K. Sunkel, U. Birk and C.Robl, *Organometallics*, 1994, **13**, 1679-1687.

59 (a) J. A. Abad, L. W. Bateman, J. C. Jeffery, K. A. Mead, H. Razay, F. G. A. Stone and P. Woodward, *J. Chem. Soc., Dalton Trans.*, 1983, 2075-2081. (b) M. R. Awang, J. C. Jeffery and F. G. A. Stone, *J. Chem. Soc., Dalton Trans.*, 1983, 2091-2098. (c) M. R. Awang, J. C. Jeffery and F. G. A. Stone, *J. Chem. Soc., Chem. Commun.*, 1983, 1426-1428. (d) S. J. Davies, A. F. Hill, M. U. Pilotti and F. G. A. Stone, *Polyhedron*, 1989, **8**, 2265-2270. (e) G. A. Carriedo, J. A. K.Howard, K. Marsden, F. G. A. Stone and P. Woodward, *J. Chem. Soc., Dalton Trans.*, 1984, 1589-1595. (f) S. J. Davies and F. G. A. Stone, *J. Chem. Soc., Dalton Trans.*, 1989, 785-795. (g) T. V. Ashworth, M. J. Chetcuti, J. A. K. Howard, F. G. A. Stone, S. J. Wisbey and P. Woodward, *J. Chem. Soc., Dalton Trans.* 1981, 763-770. (h) S. J. Dossett, A. F. Hill, J. A. K. Howard, B. A. Nasir, T. P. Spaniol, P. Sherwood and F. G. A. Stone, *J. Chem. Soc., Dalton Trans.*, 1989, 1871-1878. (i) M. D. Bermudez, E. Delgado, G. P. Elliott, N. H. Tran-Huy, F. Major-Real, F. G. A. Stone and M. J. Winter, *J. Chem. Soc., Dalton Trans.*, 1987, 1235-1242

60 B. J. Frogley and A. F. Hill, *Chem. Commun.*, 2019, **55**, 12400-12403.

61 F. G. A. Stone, *Acc. Chem. Res.*, 1981, **14**, 318-325.

62 H. J. Barnett, L. K. Burt and A. F. Hill, *Dalton Trans.*, 2018, **47**, 9570-9574.

63 (a) H. J. Barnett and A. F. Hill, *Angew. Chem., Int. Ed.*, 2020, 59, 4274-4277. (b) H. J. Barnett and A. F. Hill, *Chem. Commun.,* 2020, **56**, 12593-12596.

64 A. Reinholdt, J. E. Vibenholt, T. J. Morsing, M. Schau-Magnussen, N. E. A. Reeler and J. Bendix, *Chem. Sci.*, 2015, **6**, 5815-5823
65 L. K. Burt and A. F. Hill, *Chem. Commun.*, 2021, **57**, 8580-8483.
66 M. Millar, S. Lincoln and S. A. Koch, *J. Am. Chem. Soc.*, 1982, **104**, 288-289.
67 (a) S. Anderson, D. J. Cook, A. F. Hill, J. M. Malget, A. J. P. White and D. J. Williams, *Organometallics*, 2004, **23**, 2552-2557.
68 (a) R. D. Dewhurst, A. F. Hill and A. C. Willis, *Organometallics*, 2005, **24**, 3043–3046. (b) A. R. Delaney, B. J. Frogley and A. F. Hill, *Dalton Trans.*, 2019, **48**, 13674-13684. (c) A. F. Hill and R. A. Manzano, *Adv. Organomet. Chem.*, 2019, **72**, 103–171.
69 (a) H. Wadepohl, U. Arnold, H. Pritzkow, M. J. Calhorda, L. F. Veiros, *J. Organomet. Chem.*, 1999, **587**, 233-243. (b) C. J. Jeffery, J. A. McCleverty, M. D. Mortimer, M. D. Ward, *Polyhedron*, 1994, **13**, 353-356.
70 (a) B. J. Frogley, A. F. Hill, *Chem. Commun.*, 2018, **54**, 2126-2129. (b) A. C. Filippou, C. Wagner, E. O. Fischer and C. Vlilkl *J. Organomet. Chem.*, 1992, **438**, C15-C22. (c) A. C. Filippou, P. Hofmann, P. Kiprof, H. R. Schmidt, C. Wagner, *J. Organomet. Chem.*, 1993, **459**, 233-247.
71 J. Won, H. Jung, M. V. Mane, J. Heo, S. Kwon and M.-H. Baik, *Adv. Inorg. Chem.*, 2019, **73**, 385-443.
72 (a) J. F. Hartwig in *Organotransition Metal Chemistry* University Science Books, Sausalito, California, 2010, 421. (b) R. H. M. Crabtree in *The Organometallic Chemistry of the Transition Metals*, John Wiley & Sons, Inc., Hoboken, New Jersey, 2014, 290–316.
73 N. M. Kostic and R. F. Fenske, *J. Am. Chem. Soc.,* 1981, **103**, 4677-4685.
74 (a) R. G. Parr and W. Yang, *J. Am. Chem. Soc.,* 1984, **106**, 4049-4050. (b) P. Fuentealba, P. Pérez and R. Contrerasc, *J. Chem. Phys.*, 2000, **111**, 2544-2551.
75 (a) J. Oláh, C. van Alsenoy and A. B. Sannigrahi, *J. Phys. Chem. A,* 2002, **106**, 3885–3890. (b) R. K. Roy, *J. Phys. Chem. A* 2003, **107**, 10428–10434.
76 (a) S. Takemoto, J. Ohata, K. Umetani, M. Yamaguchi and H. Matsuzaka, *J. Am. Chem. Soc.*, 2014, **136**, 15889–15892. (b) S. Takemoto, H. Ishii, M. Yamaguchi, A. Teramoto, M. Tsujita, D. Ozeki and H. Matsuzaka, *Organometallics*, 2019, **38**, 4298–4306. (c) S. Takemoto, M. Tsujita and H. Matsuzaka, *Organometallics*, 2017, **36**, 3686–3691.